DIAGNOSIS AND REMEDY OF NONLINEARITIES IN ELECTRODYNAMICAL TRANSDUCERS

Wolfgang Klippel

www. klippel.de

Abstract - Nonlinear and thermal mechanisms in woofers, headphones, shakers and other actuators produce signal distortion and limit the acoustic output at high amplitudes. Large-signal parameters based on extended transducer modeling and measured by system identification techniques reveal the physical causes, allow an objective assessment of the performance and give indications for practical improvements. Typical problems are discussed in a case study based on a set of drivers intended for woofer application.

I. INTRODUCTION

There are a variety of subjective and objective techniques developed to assess the quality and properties of loudspeaker systems. As illustrated in Fig. 1 subjective tests are performed to measure the sensations and preferences of listeners and to extract reliable and reproducible data by statistical analysis. The subjective information about the perceived sound quality reflects the physical properties of the loudspeaker, room and music and the psycho-acoustical phenomenon as well as the cultural background of the listener. Although subjective evaluation is the ultimate criteria, the engineer relies on objective measurements to assess the physical properties of the loudspeaker. In Fig. 1 the objective measurements are separated in two classes: Measurement of the transfer response and identification of the loudspeaker model.

The first class of measurements is based on a general system approach and focuses on the behaviour of the systems under special reference conditions. In practice we excite the loudspeaker with a test stimulus and measure the linear and nonlinear distortion in the output signal.

The linear distortion deteriorates the amplitude and phase response only. Assuming a linear model the variations of sound pressure levels versus frequency are independent of the amplitude of the stimulus.

Nonlinear distortion produces new spectral components (harmonics and intermodulations) and alters the amplitude and phase of the fundamental components as well. At low amplitudes the loudspeaker behaviour is almost linear and nonlinear signal distortion is negligible. However, nonlinear distortion grows faster than the amplitude of the input signal and reaches soon substantial amplitudes. The nonlinear behaviour starts not suddenly at a critical amplitude like amplifier limiting and the nonlinearities of most loudspeakers follow a quadratic or cubic function. Some nonlinear distortion are directly correlated with cost, weight, efficiency of the driver. Others kinds of distortion indicate a design or manufacturing problem.

Nowadays, there is a growing interest in increasing the acoustical output of the driver while using the same amount of natural resources and producing acceptable distortion. New ways in passive driver design and active compensation are explored to refine the performance in the large signal domain. In this approach it is not sufficient to observe the effects of the nonlinearites by measuring harmonic and intermodulation distortion only. More detailed information about the source and the physical mechanisms are required. Recent loudspeaker research has developed extended loudspeaker models considering parameter variations at high amplitudes. New measurement techniques can identify the free parameters of the model on a particular speaker being operated under normal working condition. These parameters are the basis for numerical simulation used to predict or to analyse the behaviour of the loudspeaker. The identification technique enables the engineer to measure distortion in the reproduced audio signal and to analyse the contribution from each nonlinearity. Since the loudspeaker may be operated under normal

working conditions the results might be more relevant for the subjective evaluation. In any case this information is crucial for understanding the physical reason of the nonlinear and thermal effects and to diagnose design and to derive suggestions for constructional improvements.

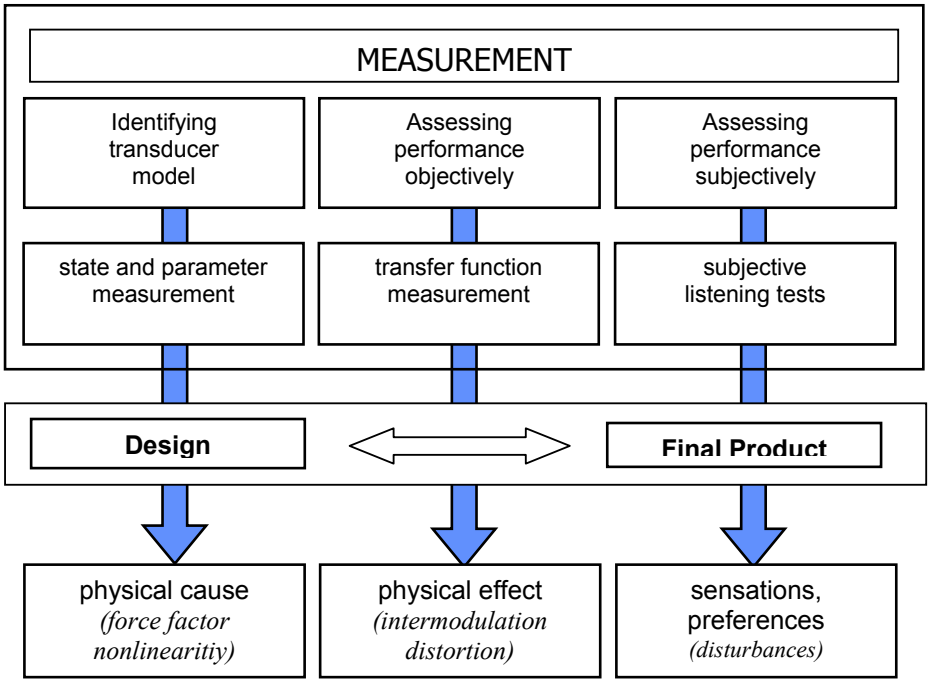

Fig. 1: Measurements in the Loudspeaker Design Process

The paper is organised as follows: After summarising the results of transducer modelling and parameter measurement the different sources of distortion are classified and the relationship to the large-signal parameters are derived. This case study is illustrated on a set of drivers intended for woofer application.

II. TRANSDUCER MODEL

At low frequencies loudspeaker drivers and other electrodynamical actuators may be modeled by an electrical equivalent circuit as shown in Fig. 2 and Fig. 3 comprising lumped elements and state quantities:

u	voltage at terminal
i	electrical input current
x	voice coil displacement
v	voice coil velocity
P	electrical input power
$F_m(x,i)$	reluctance force
T_V	voice coil temperature
T_A	ambient temperature
T_M	temperature of magnet structure
$R_E(T_V)$	electric DC resistance depending on voice coil temperature

$L_E(x)$, $L_2(x)$, $R_2(x)$	lumped elements to describe voice coil impedance
$b(x)$	electrodynamic coupling factor (effective Bl product)
$C_{MS}(x)$	mechanical compliance of driver suspension
M_{MS}	moving mass including air load
R_{MS}	resistance representing mechanical and acoustical losses
C_{TV}	thermal capacitance of voice coil
R_{TV}	thermal resistance of path from coil to magnet structure
R_{TM}	thermal resistance of magnet structure to ambient air
C_{TM}	thermal capacitance of magnet structure

The resistance $R_E(T_V)$ describes the electrical impedance of the voice coil at DC and depends on the voice coil temperature T_V. The inductance of the voice coil and the effect of eddy currents at higher frequencies is modelled by the lumped elements $R_2(x)$, $L_E(x)$ and $L_2(x)$ with

$$\frac{L_E(x)}{L_E(0)} = \frac{L_2(x)}{L_2(0)} = \frac{R_E(x)}{R_E(0)}. \qquad \textbf{(1)}$$

The dependency of $L_E(x)$ and $L_2(x)$ on x generates a reluctance force $F_m(x,i)$ on the mechanical side driving the voice coil for positive and negative currents into the inductance maximum. This mechanism is the motor in electromagnetic transducers. The nonlinear function between current and driving force is a source of distortion. Electrodynamic transducers expoits a linear relationship between electric charges in the voice coil wire and a magnetic field fixed at a local position. The coupling between electrical and mechanical domain can be modeled by a transformer with coupling constant $b(x)$. For a moving coil this coupling parameter also called force factor or effective Bl-product depends on the voice coil displacement x and summarizes the effect of voice coil geometry and penetrating magnetic induction B. The flux flowing through the gap is the superposition of a permanent field generated by the magnet and an alternating field generated by the voice coil itself.

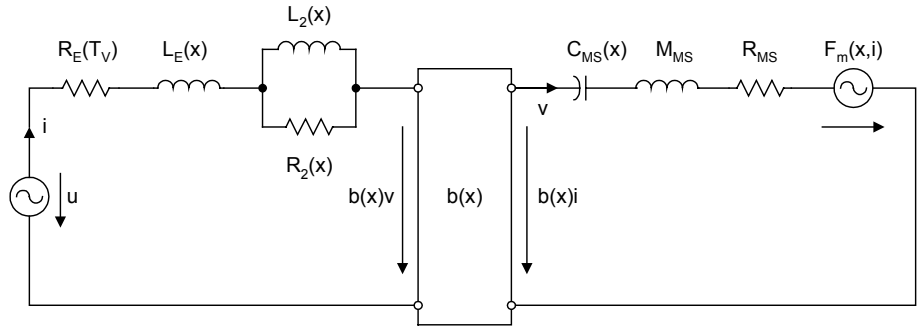

Fig. 2: Nonlinear electro-mechanical equivalent circuit of the transducer.

The mechanical and acoustical system can be represented by three lumped parameters: The moving mass M_{MS} represents the inertia of the voice coil, diaphragm, suspension and air load of the radiation. The stiffness $K_{MS}(x)$ inversely related to the compliance $C_{MS}(x)$ represents the spring constant of the suspension depending on the geometry and material of the spider and surround. All of the mechanical and acoustical losses are represented by the mechanical resistance R_{MS}. This equivalent circuit considers the dominant nonlinearities in woofer systems and neglects secondary nonlinearities such the variation of the moving

mass $M_{MS}(x)$ and the mechanical resistance $R_{MS}(x)$ versus displacement and distributed nonlinearities in the diaphragm.

Operating woofers at high amplitudes the voice coil temperature T_V will be rise from the ambient temperature T_A over time and increases the voice resistance $R_E(T_V)$. The thermal equivalent circuit shown in Fig. 3 comprises two integrators supplied with the electric input power P. The voice coil is represented by the thermal resistance R_{TV} and the capacity C_{TV} forming a first-order integrator with a relatively low time constant $\tau_{TV}=R_{TV}*C_{TV}$. The warming of the frame, magnet, pole plates and piece is modelled by the second integrator comprising the thermal resistance R_{TM} and capacity C_{TM} producing a relatively long time constant $\tau_{TM}=R_{TM}*C_{TM}$.

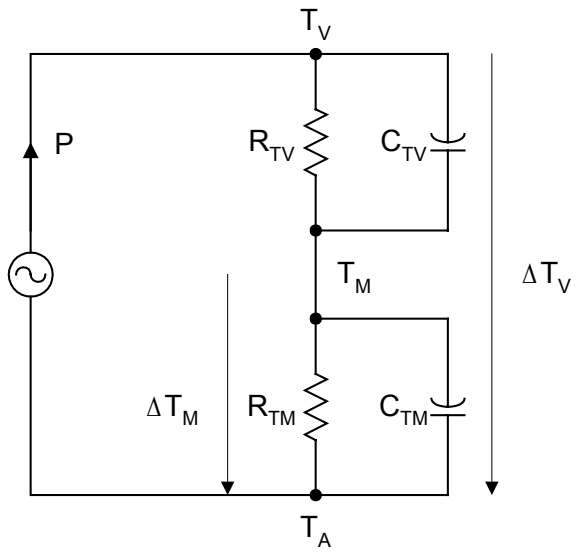

Fig. 3: Thermal equivalent circuit of the transducer.

The loudspeaker model comprises three kinds of information: The structural information is given by the equivalent circuits and the general properties of the lumped elements and is valid for many types and variations of electrodynamic transducers as long as the mechanical system can be represented by lumped parameters in the interested frequency range. The values of the constant parameters (R_{MS}, $M_{MS,\ldots}$) and the nonlinear function of the varying parameters ($b(x)$, …) represent the second class of information which have to be identified for the particular unit. Finally the state information such as the time varying quantities (displacement x, current i, power P and temperature T_v) depends on both the loudspeaker parameters and the instantaneous signal properties.

III. IDENTIFICATION OF THE LOUDSPEAKER MODEL

Special measurement techniques have been developed to estimate the loudspeaker parameters in the large signal domain.

The static and quasi-static methods use means for generating an adjustable DC-component in the displacement x to sample the working range of loudspeaker. A series of measurement is required to identify the nonlinear characteristic. These methods are time-consuming and a high DC-displacement changes the suspension properties (lower stiffness value, undefined rest position) temporally.

The Distortion Analyzer [35] performs a full dynamic measurement dispensing with a DC-component in the displacement. The loudspeaker is operated under normal conditions using an audio-like signal for

excitation. Although music can be used a noise signal as specified in the AES2-1984 or IEC 268-5 gives more persistent excitation and reduces the measurement time.

The system identification is accomplished by implementing the loudspeaker model in the digital domain. The free parameters are estimated adaptively by minimising the error between a state signal measured at the speaker and a signal predicted by the model. The electrical current *i(t)* measured at the loudspeaker terminals provides all of the required information to identify the electrical elements of the transducer model in absolute terms and the mechanical elements in relative terms. The mechanical parameters can also be identified in absolute units by importing one mechanical parameter, measuring the displacement with a laser displacement sensor or performing a second impedance measurement where the driver is combined with a enclosure or an additional mass.

The case study discussed in the following paper is based on eighth drivers (A – H) manufactured for woofers in large quantities and measured by the Distortion Analyzer.

IV. DRIVER ASSESSMENT

The parameters and states identified on the particular driver allow to assess the driver performance in respect with the following criteria:

- The acoustical output is limited by mechanical and thermal constraints. The maximal amplitude handled by the driver safely is one of the most important parameters since a loudspeaker is expected to reproduce the sound as loudly as possible.
- The efficiency of the conversion determines the amplifier requirements and provisions made to transfer the heat away from the driver.
- Nonlinearities inherent in the driver may cause unstable vibration behaviour at high amplitudes deteriorating the efficiency and generating excessive distortion in the acoustic output. The audibility of the nonlinear distortion depends on the spectral property and on the physical nature of the distortion.
- The weight, size and cost of manufacturing determine the final application.

Parameters	Unit	Driver A	Driver B	Driver C	Driver D	Driver E	Driver F	Driver G	Driver H
$R_{E\ (T_V=T_A)}$	Ohm	3,26	3,70	3,40	7,10	3,40	4,40	6,43	3,03
$L_e(x=0)$	mH	0,55	0,85	1,68	1,41	0,40	0,98	1,18	2,37
R_2	Ohm	1,36	2,21	4,12	3,21	0,95	2,31	2,52	4,83
L_3	mH	1,01	1,64	3,07	2,39	0,71	1,72	1,87	3,50
M_{MS}	gramm	15,20	7,70	23,43	11,67	13,30	5,06	9,36	22,15
R_{MS}	kg/s	0,56	0,39	1,72	1,27	0,97	0,58	1,34	1,25
$b(x=0)$	N/A	5,53	5,66	4,55	4,64	3,64	4,92	4,94	6,10
C_{MS}	mm/N	0,72	2,63	1,04	0,50	1,04	2,22	1,36	0,60
R_{TV}	K/W	1,63	2,77	1,17	2,04	5,40	5,11	2,72	1,18
R_{TM}	K/W	1,02	1,28	0,43	0,43	1,20	0,09	0,26	0,96
C_{TV}	J/K	24,40	8,30	31,20	6,50	1,90	1,91	4,96	49,00
t_{TV}	s	40	23	37	13	10	10	13	58
S_D	S_D	123	78	132	153	213	71	92	104
total weight	kg	1,60	1,30	1,50	1,05	0,95	0,75	0,90	1,10
b_{min}	%	46	46	59	73	25	30	75	34
C_{min}	%	25	25	24	24	77	25	25	45
L_{min}	%	60	54	81	64	41	47	63	50
x_{max}	mm	10,00	7,40	13,80	8,90	7,30	6,20	6,60	12,30
$n_o\ (T_V=T_A)$	%	0,37	0,50	0,09	0,30	0,56	0,58	0,19	0,16
L_{ref}	dB	87,9	89,2	81,8	87,0	89,7	89,8	84,9	84,3
V_D	cm^3	123,0	57,7	182,2	136,2	155,5	44,0	60,4	127,9
$P_{max\ (T_V=T_A+100K)}$	W	37,8	24,7	62,7	40,5	15,2	19,2	33,6	46,8

Table 1: Parameters of eight test drivers measured in the large signal domain

Maximal Input Power

Above the resonance frequency, where the motor drives the moving mass M_{AS} and little displacement is required to produce the acoustic output, the maximal signal amplitude is limited by capability of the driver to dissipate heat. The Distortion Analyzer determines the increase voice coil temperature $\Delta T_V=T_V-T_A$ by measuring the current and estimating the variations of the electric voice coil resistance $R_E(T_V)$. According to the measurement principle the detected increase ΔT_v is a mean value of the local temperature averaged over all windings.

The measurement of the real electrical input power P and voice coil temperature T_V is the basis for the identification of the thermal parameters in Fig. 3. To measure the thermal resistance R_{TV} and capacity C_{TV} of the voice coil the input power is altered in a two minute intervals. The resistance R_{TM} and capacity C_{TM} of the magnet structure is measured by performing a long-term monitoring of the loudspeaker states. The maximal input power P_{max} in the thermal equilibrium state can be calculated from the thermal parameters by

$$P_{\max} = \frac{T_{\lim}}{R_{TV} + R_{TM}}. \qquad \textbf{(2)}$$

where T_{lim} is the maximal permissible increase of mean voice coil temperature averaged over the whole coil length.

The windings outsides the gap are usually much warmer than the middle part of voice coil close to the pole tips where the conduction through the thin air gap, the radiation and forced convection based on the flowing air gives good conditions for heat transfer. Thus, the mean temperature T_{lim} of long overhang coils should be set smaller than the maximal local temperature admissible by adhesive, wire insulation and

material of the voice coil former. The manufacturer usually determines the mean temperature T_{lim} by driving the unit at the thermal limits and investigating the thermal destruction.

Taking a safe and harmless limit T_{lim}=100 K we find the input power rating P_{max} for the drivers A - H given in Table 1. The real power P_{max} is slightly smaller than the maximal nominal electrical input power P_{Emax} which is defined as the power delivered by a low impedance source providing the effective voltage u_{rms} into a resistor having the same value as the voice coil resistance R_E [1 – 2].

In addition to the maximal long-term power handling $P_{max,}$ the short-term behaviour of the voice coil can be evaluated by the thermal time constant $\tau_{TV}=R_{TV}*C_{TV}$. The voice coil should heat slowly in the first few seconds to give good transient behaviour and to protect the coil. The time constant τ_{TV} of the drivers in Table 1 ranges from 10 s to 50 s depending on the mass of the voice coil and the material of the voice coil former (aluminium, paper).

Passband Efficiency

One of the most important parameters of a transducer is the transfer ratio between the electric input power and the acoustic output power. The nominal or reference efficiency η_o in the pass-band of a loudspeaker mounted in an infinite-baffle is defined by the expression

$$\eta_o = \frac{P_A}{P_E} = \frac{\rho_o}{2\pi c} \frac{b(x=0)^2}{R_E (T_V = T_A)} \frac{S_D^2}{M_{MS}^2}. \quad \textbf{(3)}$$

with the nominal electric input power P_E, acoustic output power P_A, speed of sound in air (c=345m/s), effective projected surface area S_D of driver diaphragm, density of air (ρ_o =1.18 kg/m^3). The reference efficiency describes the cold driver at low voice coil displacement. Both an increase of the voice coil temperature and variations of the force factor will reduce the efficiency significantly. Table 1 gives the nominal efficiency η_o and the reference sound pressure level rating L_{ref} for 1 W input at a distance of 1 meter. Driver C requires almost 6 times more input power (7.9 dB) as driver F to produce the same acoustic output level.

Maximal Displacement

At low frequencies a high displacement of the diaphragm is required to produce the acoustic sound pressure level in the far field. However, both the mechanical suspension and the motor limit the maximal displacement by generating excessive distortion or causing a permanent damage of the unit. The maximal displacement is designated by x_{max} and can be derived from the nonlinear characteristics of force factor $b(x)$ and compliance $C_{MS}(x)$ objectively.

For this task we introduce the nonlinear variation of the force factor

$$b_{\min}(x_{\max}) = \min_{-x_{\max} < x < x_{\max}} \left(\frac{b(x)}{b(0)} \right). \quad \textbf{(4)}$$

and the variation of the compliance

$$C_{\min}(x_{\max}) = \min_{-x_{\max} < x < x_{\max}} \left(\frac{C_{MS}(x)}{C_{MS}(0)} \right). \quad \textbf{(5)}$$

determined by the ratio of the minimal parameter value and the value at the rest position $x=0$. As relative quantities these variations describe the nonlinearity but not the absolute value of the parameter. Both measures may be used to define of the permissible mechanical load and the safe range of operation.

Now, the maximal displacement x_{max} may be defined by the displacement x where either the compliance variation or the motor variation reach a critical limit value $C_{min}(x) = C_{lim}$ *and* $b_{min}(x) = b_{lim}$, respectively. For example, a variation b_{lim} = 50 % produces high motor distortion. A compliance variation C_{lim} = 25 % puts the suspension under substantial mechanical stress and indicates the end of the safe working range.

The Distortion Analyzer uses the values C_{lim}, b_{lim}, T_{lim} as protection parameters defined by the user as general setup parameter for a variety of drivers. They are the basis for determining the amplitude of the excitation signal used in the measurement, the maximal displacement x_{max} and maximal input power P_{max} for the particular driver, automatically.

For the eight driver in the case study the protection parameters was set to C_{lim}=25%, b_{lim}=25 % and T_{lim}=100K. After identifying the small signal parameters the gain has been slowly increased until one of the predefined limits has been reached or excessive distortion has been occurred. The final values of x_{max}, b_{min}, C_{min} are given in Table 1 and the voice coil temperature ΔT_V at the end of the measurement are shown in Table 2. The maximal displacement x limited the amplitude of the noise signal. Only the voice coil temperatures of driver D and H came close to the allowed threshold T_{lim}. The drivers A, B, C, D, F and G are limited by mechanical suspension and driver E is caused by the force factor nonlinearity. The voice coil of driver H hits at x = -12.3 mm the back-plate before the capability of the motor and suspension is exhausted.

A fundamental large-signal parameter of a driver is the diaphragm peak displacement volume defined by

$$V_D = x_{\max} S_D \ . \qquad \textbf{(6)}$$

which is directly related with maximal acoustic output at low frequencies below the resonance.

Signal Distortion

The parameters in Table 1 are the basis for predicting the linear behaviour of the driver at small amplitudes and for assessing the maximal acoustic output under simple constraints $b_{min} > b_{lim}$, $C_{min} > C_{lim}$ and $\Delta T_V < T_{lim}$. These criteria are convenient to detect the allowed working range and prevent permanent destruction but can not explain the deterioration of sound quality.

The generation of nonlinear distortion in the acoustical output depends not only on the nonlinear parameters but also on the interaction with the excitation signal. Clearly, the nonlinear parameters $b(x)$, $C_{MS}(x)$ and $L_E(x)$ will only produce a nonlinear effect if the excitation signal generates sufficient voice coil excursion. The dependency on amplitude and spectral properties make conventional distortion measurement using a two-tone excitation signal to a time-consuming task: The frequency and amplitude of the tones has to be varied in all possible combinations to measure the driver's behaviour completely. The final spectral analysis produces a large amount of data which have to be interpreted. In practice harmonic and intermodulation are measured under special conditions and the measured data are used as indication of the nonlinear mechanisms only.

New advanced techniques have been developed to measure the distortion generated by a broadband signal such as music or noise. The correlation techniques measures the incoherence between the input and output signal which is a measure for the nonlinearity of the driver. Alternatively, the identified loudspeaker model may be used to simulate the nonlinear behavior for an artificial or real audio signals. Since the Distortion Analyzer uses a digital implementation of the loudspeaker model the nonlinear distortion components produced by the dominant nonlinearities are calculated on-line and are available for statistical and spectral analysis. Simple measures of distortion are the ratios d_b, d_C, d_L defined as the peak value of distortion components generated by $b(x)$, $C_{MS}(x)$ and $L_E(x)$, respectively, related to the peak value of the total output signal.

State	Unit	Driver A	Driver B	Driver C	Driver D	Driver E	Driver F	Driver G	Driver H
P	W	20	4,9	21	31	9,3	3,52	7,38	36
DT_V	K	53	20,5	40	82	64	18,3	22,3	83
PC	dB	-1,6	-0,65	-1,22	-2,4	-1,84	-0,58	-0,71	-2,37
i_{peak}	A	6,6	3,6	8,5	5,5	4,6	2,5	3,2	8,7
u_{peak}	V	36	18,5	55	61	24	18,9	28	63
d_C	%	45	29	46	78	12	34	46	23
d_B	%	20	38	18	4,5	68	49	7	35
d_L	%	7	15	5,5	7	9	13	6	36

Table 2: States of the Drivers under test in the large signal domain

Table 2 shows the distortion ratios for the drivers A – H operated in the full operation range defined by x_{max} and the state parameters

ΔT_V	increase of voice coil temperature,
P	electric input power,
PC	thermal power compression factor describes the loss of efficiency due to voice coil heating at frequencies where the resistance R_E dominates the total electric input impedance,
i_{peak}	peak value of the electric input current,
u_{peak}	peak value of the electric voltage at the transducer terminals.

The force factor distortion d_B and suspension distortion d_C correlate approximately with the nonlinear variations b_{min} and C_{min}, respectively. However, the suspension distortion of drivers with the same C_{min} tends to rise with the resonance frequency. According to the relative definition of distortion measures the value of d_C will fall if the spectral content of the excitation signal at higher frequencies will be increased but the force factor distortion d_B will stay almost constant. The nonlinear inductance distortion d_L depends from the interaction of L_{min}, the absolute value of the inductance and the amplitude of the input current i. Thus, the driver H having a low voice coil resistance R_E= 3 Ohm and extremely high absolute variation of $L(x)$ produces high distortion d_L. This value grows by increasing the upper frequency limit of the driver's transfer band. Thus loudspeaker H should be used at low frequencies only. The driver D is an example for a driver having a very nonlinear suspension and a linear motor producing distortion components at low frequencies (below 200 Hz) only. This loudspeaker is ideal for reproducing a high frequency band at high quality. The driver E has the most linear suspension but generates the highest value of force factor distortion d_B which comprise mostly intermodulation effecting the whole spectrum of the excitation signal.

Variance of loudspeaker parameters

The total loss factor Q_{TS} considering all system resistances and the resonance frequency f_S are important parameters for the final alignment of the loudspeaker system. Both parameters vary with the displacement if the motor and the suspension are nonlinear.

The instantaneous value $f_S(x)$ is proportional to the square root of stiffness $K_{MS}(x)$. Operating the driver A,B, C, D, F and G at x_{max} where C_{min}=25% the resonance frequency is shifted one octave higher then at the rest position $x=0$.

An increase of the resonance frequency f_s also leads to a higher mechanical loss factor Q_{MS} and has also an effect on the total loss factor Q_{TS}. However, the electrical damping usually dominates and variations of $Q_{TS}(x)$ can be neglected if the motor is sufficiently linear.

Contrary, the electrical damping of the system will vanish with the squared force factor variation. For example, if the force factor variation goes down to B_{min}= 25% the electrical loss factor $Q_{ES}(x_{max})$ increases by factor 16 and the remaining mechanical damping will determine the total Q_{TS}. Operating driver F at x_{max} the total Q_{TS} is 10-times higher than at the rest position giving more acoustic output at f_s. However, the generation of a distinct resonance peak and the shift of the resonance frequency by one octave are usually perceived as a spectral coloration of the sound (booming bass).

Stability

At high amplitudes the nonlinearities cause an complicated behaviour indicating that the normal working mode becomes unstable.

For example, a driver having a distinct nonlinearity in the suspension and a high total Q_{TS} may work in two different states producing a high and a low displacement for same electrical excitation. A bifurcation is said to have occurred and the state depends on the way the drivers is lead to this state.

Another effect of instability is the dynamic generation of a DC-component in the voice coil displacement. It is well known that any asymmetry in the nonlinear parameters will rectify the signal and will generate a DC-component. Norris [17] showed that also a driver with perfectly symmetrical nonlinearities might also behave unstable and the coil moves out of the gap under certain conditions. Anyway, this effect produces not only substantial second- and higher-order distortion but will also reduce the efficiency of the driver.

Displacement	Unit	Driver A	Driver B	Driver C	Driver D	Driver E	Driver F	Drivr G	Driver H
x_{peak}@20 Hz	mm	5,6	9,4	13,2	4,3	7,3	6,5	7,2	12,5
x_{bottom}@20 Hz	mm	-5,0	-6,1	-11,2	-5,6	-7,9	-4,8	-5,3	-11,9
x_{DC}@20 Hz	**mm**	**0,3**	**1,7**	**1,0**	**-0,7**	**-0,3**	**0,9**	**1,0**	**0,3**
x_{peak}@$f=f_s$	mm	5,2	8,6	12,5	5,9	7,6	6,5	7,2	11,7
x_{bottom}@$f=f_s$	mm	-4,7	-5,9	-11,2	-6,8	-7,4	-5	-5,6	-10,8
x_{DC}@$f=f_s$	**mm**	**0,25**	**1,35**	**0,65**	**-0,45**	**0,1**	**0,75**	**0,8**	**0,45**
x_{peak}@f=150Hz	mm	1,7	-0,56	0,8	1,3	1,6	-0,3	1,7	0,3
x_{bottom}@f=150Hz	mm	-1,6	-5,8	-3,5	-1,8	-0,6	-5,5	-1,75	-4,2
x_{DC}@f=150 Hz	**mm**	**0,05**	**-3,18**	**-1,35**	**-0,25**	**0,5**	**-2,9**	**-0,025**	**-1,95**

Table 3: Stability of voice coil position measured for three sinusoidal tones by using the Distortion Analyzer as laser sensor

The DC-generation of the drivers in the case-study is measured by using the Distortion Analyzer as a laser displacement meter.

Table 3 shows the peak displacement x_{peak}, the bottom displacement x_{bottom} and the DC-displacement ($x_{DC}=(x_{peak}+x_{bottom})/2$) for three excitation frequencies f_1 = 20Hz, $f_2 = f_s$ and f_3 = 150 Hz. All of the drivers produce a positive or negative DC- component depending on the excitation frequency and on the particular properties of the nonlinear parameters. For $f \leq f_s$ the DC-components are usually small. Only driver B produces a value which exceeds 20 % of the AC-amplitude. At frequencies above the resonance frequency the instability becomes generally worse and the voice coil jumps out of the gap. The DC-component of drivers B, F, equals the amplitude of the AC-signal. In this working point the force factor is reduced to half of the value $b(x=0)$ at the rest position and the driver will only have 25% of the reference efficiency.

The generation of a DC-component is a deterministic process which can be explained by the relationship between the dominant nonlinear parameters force factor, stiffness and inductance and the spectral properties of the excitation signal. Each kind of nonlinearity generates a contribution to the DC-

component depending on the phase and amplitude of the state signals multiplied in the nonlinear terms of the differential equation.

The nonlinear stiffness generates a restoring force which is a power function of displacement only. This nonlinearity can only generate a significant DC-component at low frequencies because the amplitude of x falls above the resonance frequency with 12dB per octave. This DC-component moves the coil for all input signals into the minimum of the stiffness characteristic.

Variations of the force factor change the electric damping and the electrodynamic driving force. The nonlinear damping is the product of velocity and a power function of displacement. This term can not generate a DC component because both signals are orthogonal to each other (90^0 out of phase) and the product will vanish in the mean. The electrodynamic driving force generates a DC-component depending on the phase relationship between electric current i and power function of displacement x. At low frequencies the DC component tends to move the voice coil into the maximum of the force factor curve. Since the asymmetry of the motor is partly removed the DC-component reduces the amplitude of the higher-order distortion. At the resonance frequency $f=f_s$ no DC-component is generated by the force factor nonlinearity because the current i and displacement x become orthogonal to each other. For excitation tones above the resonance frequency the generated DC-component tends to move the voice coil away from the force factor maximum. This effect increases the asymmetry and causes the instability of drivers B and F.

The nonlinear inductance causes two effects, namely the self-induced voltage on the electrical side and the reluctance force at the mechanical side. However, the induced voltage can not generate a DC component because the total flux is differentiated and any DC-component will be removed by the differentiator. The reluctance force is a function of the squared current and the local gradient of the inductance and generates a DC-component moving the voice coil into the maximum of the inductance. The DC-component of the reluctance force becomes negligible at f_s due to the high impedance value and the small voice coil current i.

Excitation Tone	**Dominant source for generation of DC-component**	**DC-component generated by motor**	**DC-component generated by suspension**	**DC-component generated by reluctance force**
$f < f_s$	Asymmetry of suspension	moves coil to $b(x)$ maximum	moves coil in stiffness minimum	moves coil in $L_e(x)$ maximum
$f = f_s$	Asymmetry of suspension	= 0	moves coil in stiffness minimum	negligible
$f > f_s$	Asymmetry or symmetrical variation of force factor	moves coil away $b(x)$ maximum (unstable)	negligible	moves coil in $L_e(x)$ maximum
$f >> f_s$	Asymmetry of inductance	negligible	negligible	moves coil in $L_e(x)$ maximum

Table 4:Source for generating a DC component in voice coil displacement

Table 4 summarizes the relationship between the physical causes and generated DC-component for four different excitation tones. After making a displacement measurement for a few excitation tone this information can be used to identify the physical cause of the DC-generation by undergoing the following steps:

1. The DC-component generated at the resonance frequency shows the direction of the stiffness minimum. For example, all drivers in our case study besides the driver D have a stiffness minimum at positive displacements. The results of the laser measurement in Table 3 coincide with the nonlinear parameters given in the appendix.

2. The DC-component generated by a sinusoidal tone $f \approx 3f_s$ shows the combined effect of stiffness, force factor and inductance. However, a small force factor asymmetry may produce a substantial DC-component.
3. The DC-component at high frequencies is usually small indicating that the reluctance force is almost negligible.

Recommended Application

The differences in physical properties, price and weight make the particular driver preferable for a special application.

The driver D and G are based on a most linear motor design producing lowest intermodulation at high frequencies. Both drivers are optimal for high-quality woofers operating up to a high cross-over frequency.

Contrary, the drivers B, E and F use a nonlinear motor giving highest efficiency in the pass-band. These drivers produce maximal acoustic by using minimal amount of energy and material. These loudspeakers have the lowest values in power handling capacity P_{max} and a short thermal time constant for heating up the voice coil. Such loudspeakers are optimal for the combination with a digital control system to compensate for intermodulation distortion actively.

Driver C produces maximal volume velocity V_D by realising a high value of x_{max} . This driver has the lowest efficiency but has the largest power handling capacity P_{max} to dissipate heat.

V. DIAGNOSIS

The nonlinear characteristics of the loudspeaker parameters show the physical cause of the nonlinear distortion. This information is crucial to evaluate the geometry and material used in loudspeaker design, to investigate the interplay of all components in the final product, to identify assembling problems and finally to improve the driver in respect with the following criteria

1. Robustness against mechanical overload
2. System stability
3. High acoustic output
4. Minimal distortion
5. Low hardware effort

Mechanical robustness is the first target in a good driver design. Since, most of the drivers are still operated without electronic means for mechanical protection, this feature determines the durability of the driver under harsh working condition. A driver is expected to withstand overload to a certain extent without causing a permanent destruction of the unit. Robustness can be improved by designing self-protecting capabilities. For example, the moving capability of the voice coil should be limited by the suspension but not by the back-plate (as driver H does), the length of the leads or by rubbing at the pole tips.

Also the suspension system needs some attention. Excessive mechanical stress may cause a damage in long-term use. Distributing the mechanical load on a larger area is a way to improve the mechanical robustness.

A stable vibration behaviour at high amplitudes is the second step in the loudspeaker optimisation. The causes of the instability have to be tracked down and the constructional problem has to be fixed before optimising output, distortion and hardware requirement.

The third step in loudspeaker optimisation explores the mechanisms which limit the acoustic output. If a driver is limited by the suspension a more powerful motor will not give much more x_{max} but might destroy the suspension. On the other side it is not very efficient to combine a weak motor having a low b_{min} with a linear suspension.

In the fourth step the designer copes with the driver nonlinearities which do not require a compromise in large signal parameters x_{max}, f_s, P_{max}, η_o, manufacturing cost, size and weight. Most of the asymmetries in the loudspeaker characteristics can be reduced at low cost giving minimal second- and higher-order distortion and improved stability. After fixing the primary problems the force factor and compliance variations, b_{min} and C_{min}, respectively, are mainly caused by symmetrical parameter variations.

In the last step the balance between final performance and effort is evaluated and compared with the target values defined for the intended application.

Nonlinearities of the Suspension

The nonlinear characteristic of stiffness $K_{MS}(x)$ or compliance $C_{MS}(x)$ versus displacement x describes the effect of surround and spider combined to the total suspension system as shown in Fig. 4. The properties of the spider may be separated from the influence of the surround by cutting away most of the surround material except residual bridges giving sufficient guidance for a dynamic measurement with the Distortion Analyzer. However, even a non-destructive measurement of the total system gives sufficient clues about the origin of the suspension problem.

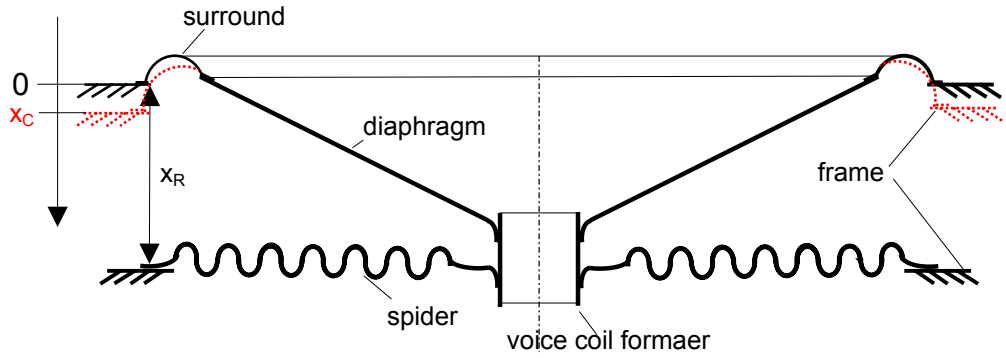

Fig. 4: Suspension System

A spider is typically made from resin impregnated cloth (blends of cotton, polyester, aramids) attached between the frame and the voice coil former. The profile of spider namely the geometry of the foots required for fastening and the corrugation rolls pressed into cloth have major influence on the linearity of the spider.

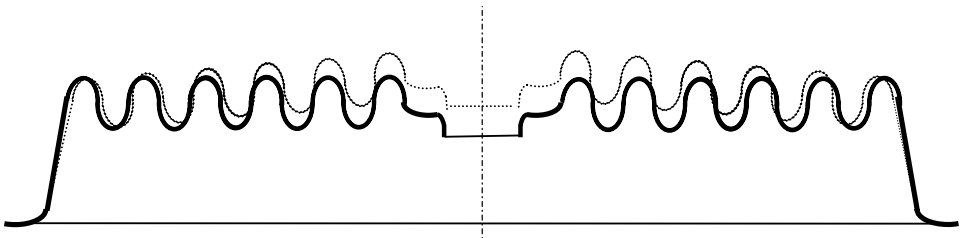

Fig. 5: Cup spider with constant roll geometry

The asymmetrical geometry of cup spider having a final roll as illustrated in Fig. 5 causes an asymmetrical stiffness characteristic. Driver G is a typical example having a stiffness minimum at x=1,5 mm as shown Fig. 54 and generating a positive DC-component x_{DC} = 1 mm at low frequency as shown in Table 3. Fortunately, the DC-component will not deteriorate the symmetry and stability of the motor because the driver G uses a high voice coil overhang. However, combining such a cup spider with a nonlinear motor having a symmetrical *b(x)* characteristic as in Fig. 39 the resulting system might become unstable. An initial small DC-component caused by the suspension lets the voice coil work on the right slope of the *b(x)*-characteristic and the rising force factor asymmetry will substantially enhance the DC-component for $f > f_s$. The asymmetry of cup spiders is a topic for further research. It seems that this phenomenon may be related to the memory of the resin/fibre structure causing the creep effect. After switching off a high amplitude signal the stretched fabric of the spider will take some time to contract to the original profile. The stretched and longer corrugation area will cause an asymmetrical deflection of the profile shown as dotted line in Fig. 5.

The stiffness characteristic of a spider with a flat profile as shown in Fig. 4 is almost symmetrical if the number of grooves equals the numbers of ridges or there are enough corrugation rolls. The symmetrical increase of stiffness with positive or negative displacement corresponds with the spider dimension (inside and outside radius) and the geometry of the corrugation rolls. In addition to the standard spider having rolls of equal size the progressive and regressive spiders have a varying roll height and spacing increasing and decreasing with the radius as illustrated in Fig. 6 and Fig. 7, respectively.

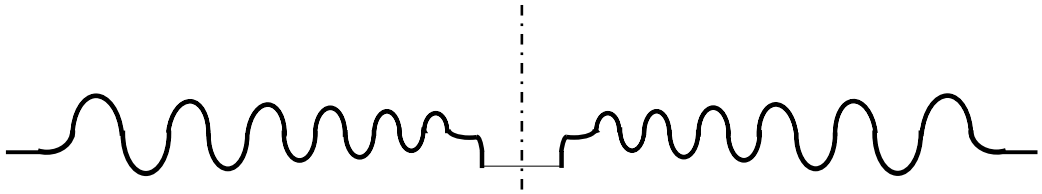

Fig. 6: Flat spider with progressive roll geometry

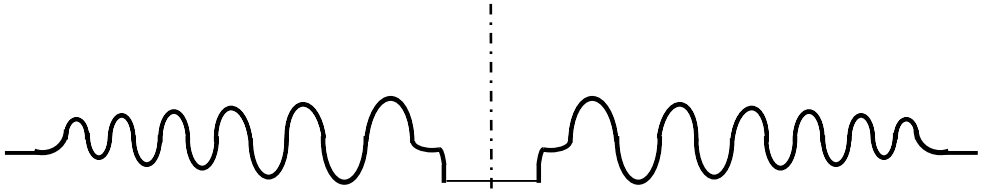

Fig. 7: Flat spider with regressive roll geometry

Hutt [34] compared the different profiles and found that the regressive spider gives a better distribution of stress in the inner rolls resulting in extended linear excursion. Contrary, the progressive spider gives more

symmetrical increase of the stiffness than the standard profile. This produces more distortion at low frequencies but might be a desired feature for a very soft suspension to protect the voice coil against mechanical damage. Standard, progressive or regressive spiders with a normal number of rolls, typically 5 –10, have a smooth nonlinear characteristic where the increase of stiffness starts gradually at small amplitudes. Spiders having 1 – 3 rolls only as used for miniature, midband or tweeter systems show a rapid increase at higher amplitude indicating high stress in the material and the end of the moving capability.

The linearity of the surround also depends on the material and its geometry. Surrounds made of paper or cloth with many corrugation rolls as used in drivers for professional application have similar properties as a spider.

Surrounds made of soft rubber and foam material contributes not much to the total stiffness at low amplitudes. However, the stiffness increases rapidly if the material is stretched and the moving capability of the surround is exhausted. High stress in foam material reduces the durability of the system and should be avoided. The driver B is a typical example where the surround causes an asymmetrical limiting. Here reducing the distance x_r between frame and surround by x_C = 2 mm as shown in Fig. 4 will fix the problem at low cost.

Fig. 47 shows the stiffness characteristic of driver F where the surround limits both negative and positive excursions. A small asymmetry can be corrected by increasing the distance x_r. The optimal change of x_r can be derived from the parameter $x_c(x)$ describing the symmetry point where a negative and positive displacement x will produce the same compliance value

$$C_{MS}\left(x_C(x) + x\right) = C_{MS}\left(x_C(x) - x\right). \quad (7)$$

For driver F the symmetry point x_C is almost independent on x as shown in Fig. 51 and a shift by x_C = 0. 6 mm would give a good symmetry for all amplitudes. However, the remaining symmetrical variations at high amplitudes indicate high stress in the surround. Increasing the size of the surround or using a stiffer spider will improve durability of the suspension.

If the material used for the surround is relative hard and the stiffness of the surround at the rest position is not negligible in comparison to the stiffness of the spider then the geometry of the surround is important. A simple half wave ridge as frequently used is a source of asymmetry. The assembling of spider and surround may also introduce a pre-stress (bias) in both parts resulting that the total stiffness is not minimal at rest position x = 0 mm.

The symmetry point $x_C(x)$ versus amplitude x is a convenient tool to balance the asymmetry of spider and surround and to find a compromise where the final suspension produces minimal DC-generation in the intended working range. For example, Fig. 33 shows an asymmetrical stiffness of driver D caused by the surround at small amplitudes. Fig. 37 reveals that the suspension becomes more symmetrical at higher amplitudes due to the growing influence of the spider. The interplay between spider and surround can be improved by increasing the distance x_r by 1mm.

Table 5 summarises the relationship between physical cause and distinctive marks in the large signal parameters and give suggestions for possible improvements.

Physical Cause	Indication	Remedy	Example
• asymmetry of spider geometry (cup form)	• asymmetrical variations of $K_{MS}(x)$ starting at small amplitudes ($\|x\| \approx 0$) • optimal working point of suspension $x_C(x) \approx$ const.	• use flat spider • compensate spider asymmetry by offset of surround x_R	Speaker G
• asymmetrical geometry of surround (half wave corrugation)	• asymmetrical variations of $K_{MS}(x)$ starting at small amplitudes ($\|x\| \approx 0$)	• use grooves and ridges • increase number of corrugations	Speaker D
• asymmetrical limiting of surround	• asymmetrical variations at high amplitudes ($\|x\| \approx \|x_{max}\|$)	• change distance x_R between suspension and spider by x_C	Speaker B
• symmetrical limiting of spider	• symmetrical variations of $K_{MS}(x)$ starting at small amplitudes ($\|x\| \approx 0$)	• increase number of rolls in spider • increase size of rolls • use regressive roll geometry	Speaker C
• symmetrical limiting of the surround	• symmetrical variations at high amplitudes $\|x\| \approx \|x_{max}\|$	• increase size of roll	Speaker F

Table 5: Typical problems of the suspension system

Force Factor Nonlinearity

The force factor describes the effective coupling between mechanical and electrical parameters of the transducer. It summarises the interactions between moving electrical charges and a magnetic field generated by a permanent magnet and the current in the voice coil. The effect of the magnetic AC-field generated by the coil itself on the electrodynamic coupling is called flux modulation. It requires a resting material such as iron (pole plate, pole piece) to generate a relative movement between charges in the coil and AC-flux bound to a fixed local position. Please note that the alternating flux involved in eletrodynamic coupling is only a part of the total AC-flux generated by the voice coil. Thus, the electrodynamic force generated by the AC-field is different from the reluctance force generated by displacement-varying inductance $L_E(x)$. In most drivers flux modulation can be neglected but in drivers having a high voice coil inductance and a low induction B this mechanisms has an impact on the effective $b(x)$-characteristic.

The variation of the force factor depends on the magnetic field distribution represented by the total flux density B (induction) and on the geometry of the coil. The voice coil height h_{coil} and the height h_{gap} of the gap determine the symmetrical variations of the force factor mainly. The asymmetry of the force factor depends on the rest position of the voice coil, the geometry of the pole tips, the distance between coil and permanent magnet, and parameters involved in flux modulation (total inductance, voice coil height, pole plate thickness, …).

Assuming a motor having an overhang configuration ($h_{coil} > h_{gap}$) with ideal properties (no asymmetries, no flux outside gap) the voice coil height h_{coil} equals the peak-to-peak displacement where the force factor decrease to 50 %. The voice coil overhang $x_{lin} = h_{coil} - h_{gap}$ corresponds with the peak-to-peak displacement describing the linear excursion range where $b(x) \approx b(x=0)$. The force factor characteristics of drivers A and D, shown in Fig. 11 and Fig. 32, respectively, come very close to this ideal but most of

the drivers have substantial asymmetries. Like for the suspension asymmetry it is useful to introduce a symmetry point $x_b(x)$ defined by

$$b\left(x_b(x)+x\right) = b\left(x_b(x)-x\right) \tag{8}$$

and giving the same force factor value for negative and positive displacement x. If this point $x_b(x) \approx const.$ then the asymmetry can easily be fixed for all signal amplitudes by shifting the rest position of the voice coil by the value x_b as illustrated in Fig. 8.

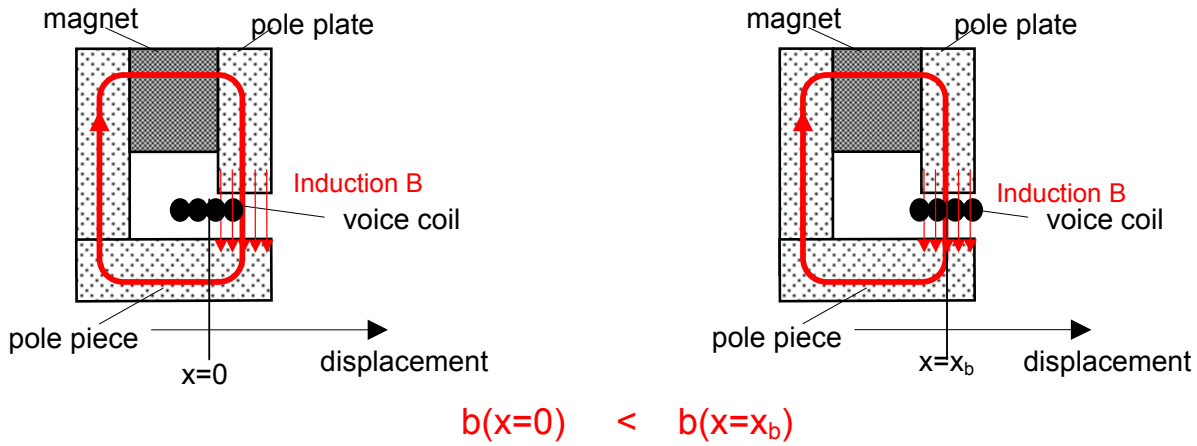

Fig. 8: Optimal rest position of voice coil

In the case study, the force factor asymmetry of driver F as shown in Fig. 46 causes a high negative DC-component for $f > f_s$ as shown in Table 1. This problem can be fixed at low cost by simply shifting the voice coil by $x_b = 1$ mm in positive direction. The optimal value can be derived from Fig. 52. The symmetry point goes down to 0.7 mm at high amplitudes due to the magnetic field geometry but it is more important to symmetrize the motor at small displacement where the motor instability starts.

Contrary, the driver C represents the case where a force factor asymmetry can not be simply compensated by a voice coil shift. Fig. 25 shows a force factor characteristic of a motor having sufficient voice coil overhang (15mm) but a substantial asymmetry caused by flux modulation due to high inductance and large gap depth h_{gap}. The symmetry point x_b as shown in Fig. 31 varies from $x_b = 6 - 2mm$. This problem can be solved by applying means for reducing the voice coil inductance.

The optimal rest is critical in motors using an equal-length configuration such as in B, E, and H . The $b(x)$ characteristic of Driver E shown in Fig. 39 is an example for a well-made equal-length configuration producing low DC-displacement at $f > f_s$.

The Table 6 gives a summary on the dominant problems related to force factor nonlinearities, there representation by the nonlinear parameters and suggestions for improvements.

Physical Cause	Indication	Remedy	Example
• voice coil is not in optimal rest position	• asymmetrical variation of force factor *b(x)*, • $x_b(x) \approx const.$	• shift rest position of voice coil by x_b	Driver F
• alternating magnetic flux generated by voice coil current	• asymmetrical variation of force factor *b(x)*, • $x_b(x) \neq const.$	• reduce alternating flux in gap by applying means for decreasing voice coil inductance (short cut ring) • reduce number of voice coil windings in gap by decreasing plate height	Driver C
• asymmetrical distribution of permanent field	• asymmetrical variation of force factor *b(x)* at higher amplitudes $\|x\| \approx \|x_{max}\|$ • $x_b(x) \neq const.$	• change pole piece to have symmetrical gap geometry • increase distance between magnet and coil	
• motor with equal-length configuration (giving higher efficiency but lower linearity)	• symmetrical decay of *b(x)* starting at small amplitudes *($\|x\| \approx 0$)*	• reduce height of pole plate • increase height of voice coil	Driver E
• motor with overhang configuration (giving lower efficiency but more linearity)	• symmetrical decay of b(x) starting at high amplitudes *($\|x\| > 0$)*	• enlarge height of pole plate to increase efficiency	Driver D

Table 6: Typical problems of the electrodynamical motor

Inductance Nonlinearity

The inductance of the voice coil describes the total magnetic flux generated by the voice coil current. If the driver is not equipped with additional means for reducing this flux the inductance varies in a characteristic way with the displacement x. As shown in Fig. 9 the air path and the magnetic resistance for negative displacement x_1 is much smaller than for positive displacement x_2 resulting in a higher flux and inductance.

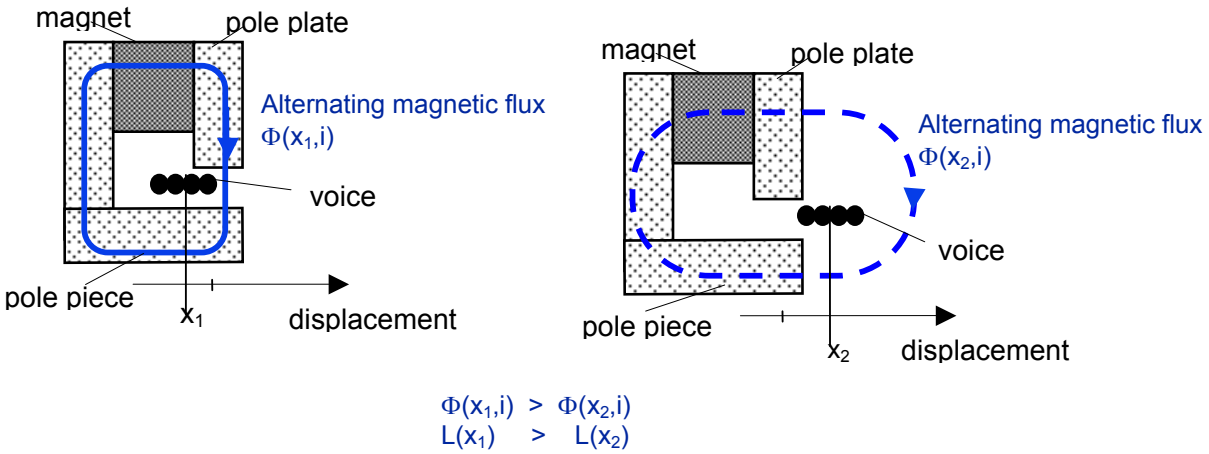

Fig. 9: Dependency of Electrical Inductance on voice coil position (without using short cut ring)

This behaviour show the drivers B-H in our case study. As discussed before the amount of inductance distortion d_L in the output signal depends not only on the variation of the inductance L_{min} but also on the amplitude of the current, the absolute inductance value and the frequency of the distortion. Therefore, driver H produces significantly higher distortions than the other drivers in the case study.

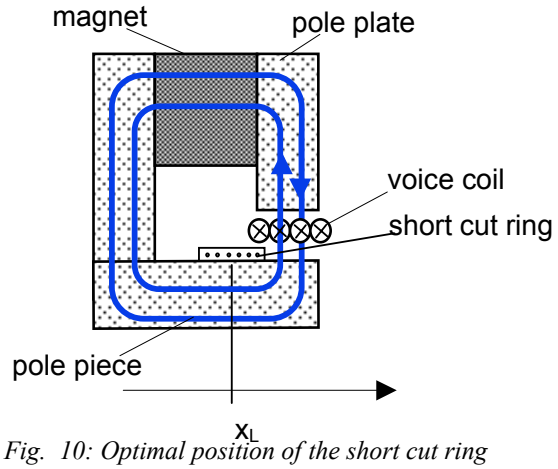

Fig. 10: Optimal position of the short cut ring

A simple but effective way to reduce this kind of distortion is to place a short cut ring or a cup over the pole piece as shown in

Fig. 10. The alternating AC-flux generated by the voice coil current induces a voltage in the ring. Using a ring material having a low electrical resistance (e.g. copper) the flowing ring current will produce a flux in the iron path in almost equal magnitude as the flux generated by the current but in opposite direction. Thus reduces the total flux and the inductance significantly. However, this compensation depends on the distance between coil and ring and optimal position x_l is critical for the linearization of the L(x)-characteristic.

Driver A shows a case where the short cut ring is more effective for negative than for positive displacements producing an abnormal characteristic as shown in Fig. 13. Shifting the ring in the maximum of the voice coil inductance (positive direction) will give a higher reduction and more linearity.

Table 7 summarises the typical inductance nonlinearities and gives suggestions for constructional improvements.

Physical Cause	Indication	Remedy	Example
• natural voice coil/gap configuration generates asymmetric L(x) characteristic	• voice coil inductance $L_E(x)$ increase with negative displacement $dL_E(x)/dx < 0$ • variations $\|dL_E(x)/dx\|$ is maximal at rest position	• use short cut ring or copper cap on pole piece • decrease absolute value of inductance by reducing number of windings	Driver B- H
• asymmetrical overcompensation of voice coil inductance	• voice coil inductance $L_E(x)$ increase with positive displacement $dL_E(x)/dx > 0$	• shift short cut ring in maximum of inductance	Driver A
• symmetrical overcompensation of voice coil inductance	• voice coil inductance has a minimum	• increase distance between short cut ring and voice coil • increase height of short cut ring • use short cut cap on pole piece	

Table 7: Typical problems of the voice coil inductance

VI. CONCLUSION

Transducers with almost identical properties at low amplitudes might behave quite differently in the large signal domain. Thermal and nonlinear parameters are the basis for assessing the performance, predicting the behaviour at higher amplitudes and explaining the physical causes. These parameters can be measured on a particular driver under normal working conditions by applying system identification techniques (Distortion Analyzer).

This information is crucial for the system designer to select the optimal driver for the particular application. The traditional large signal parameters power handling capacity P_{max} and maximal displacement x_{max} can be measured more precisely by considering the short-term and long-term heating process, the mechanical load in the suspension and the generation of the nonlinear distortion. The compliance and force factor variation C_{min} and b_{min}, respectively, are useful single value representations of the driver nonlinearities showing the dominant factors that limit acoustic output. The variation of the total loss factor and resonance frequency versus voice coil displacement have to be considered in the system alignment. The nonlinear parameters reveal the cause of unstable vibration behavior. Finally, the results of the distortion analysis show the contribution of each nonlinearity under normal working conditions.

The driver designer is interested in the details of the nonlinear parameter characteristics. Suspension asymmetries starting at small or high amplitudes give clues about limiting factors caused by material and geometry. The force factor asymmetries are mainly caused by an offset in the voice coil rest position and by asymmetries in the magnetic field distribution. The inductance asymmetries correspond with the voice coil position in the gap. All parameter asymmetries can be reduced at low cost giving improved stability, lower distortion and durability. Symmetrical variations which are directly related to efficiency, weight and cost should be dominant in a well made driver.

The large signal parameters are also the basis for predicting the transfer behaviour of a driver mounted in a enclosure and excited by a synthetic measurement stimulus or an audio-like signal. Numerical

simulation can give a deeper insight into the complex mechanisms between stimulus and nonlinear driver. They can substitute time-consuming measurements and give more relevant information for the subjective listening impression.

VII. REFERENCES

[1] R. H. Small, „Direct-Radiator Loudspeaker System Analysis," J. Audio Eng. Soc., vol. 20, pp. 383 – 395 (1972 June).

[2] R.H. Small, „Closed-Box Loudspeaker Systems, Part I: Analysis," J. Audio Eng. Soc., vol. 20, pp. 798 – 808 (1972 Dec.).

[3] A. N. Thiele, „Loudspeakers in Vented Boxes: Part I and II," in Loudspeakers, vol. 1 (Audio Eng. Society, New York, 1978).

[4] J. R. Ashley and M. D. Swan, „Experimental Determination of Low-Frequency Loudspeaker Parameters," in Loudspeakers, vol.1 (Audio Eng. Society, New York, 1978).

[5] R. H. Small, "Assessment of Nonlinearity in Loudspeakers Motors," in IREECON Int. Convention Digest (1979 Aug.), pp. 78-80.

[6] M.R. Gander, " Moving-Coil Loudspeaker Topology as an Indicator of Linear Excursion Capability," in Loudspeakers, vol.2 (Audio Engineering Society, New York, 1984).

[7] A. Dobrucki, C. Szmal, "Nonlinear Distortions of Woofers in Fundamental Resonance Region," presented at the 80th convention Audio Eng. Soc., Montreux, March 4-7, 1986, preprint 2344.

[8] C. Zuccatti, "Thermal Parameters and Power Ratings of Loudspeakers," J. Audio Eng. Soc., vol. 38, pp. 34 – 39, (Jan./Feb. 1990).

[9] D. Button, "A Loudspeaker Motor Structure for Very High Power Handling and High Linear Excursion," J. Audio Eng. Soc., vol. 36, pp. 788 – 796, (October 1988).

[10] C. A. Henricksen, "Heat-Transfer Mechanisms in Loudspeakers: Analysis, Measurement, and Design," J. Audio Eng. Soc., vol. 35, pp. 778 – 791, (October 1987).

[11] W. Klippel, "Dynamic Measurement and Interpretation of the Nonlinear Parameters of Electrodynamic Loudspeakers," *J. Audio Eng. Soc*., vol. 38, pp. 944 - 955 (1990).

[12] E. R. Olsen and K.B. Christensen, "Nonlinear Modeling of Low Frequency Loudspeakers - a more complete model," presented at the 100th convention Audio Eng. Soc., Copenhagen, May 11-14, 1996, preprint 4205.

[13] M.H. Knudsen and J.G. Jensen, "Low-Frequency Loudspeaker Models that Include Suspension Creep," *J. Audio Eng. Soc.,* vol. 41, pp. 3 - 18, (Jan./Feb. 1993).

[14] A. Dobrucki, "Nontypical Effects in an Electrodynamic Loudspeaker with a Nonhomogeneous Magnetic Field in the Air Gap and Nonlinear Suspension," *J. Audio Eng. Soc.,* vol. 42, pp. 565 - 576, (July./Aug. 1994).

[15] A. J. M. Kaizer, "Modeling of the Nonlinear Response of an Electrodynamic Loudspeaker by a Volterra Series Expansion," *J. Audio Eng. Soc*., vol. 35, pp. 421-433 (1987 June).

[16] W. Klippel, "Nonlinear Large-Signal Behavior of Electrodynamic Loudspeakers at Low Frequencies," *J. Audio Eng. Soc*. , vol. 40, pp. 483-496 (1992).

[17] J.W. Noris, "Nonlinear Dynamical Behavior of a Moving Voice Coil," presented at the 105th Convention of the Audio Engineering Society, San Francisco, September 26-29, 1998, preprint 4785.

[18] W. Klippel, " The Mirror Filter - A New Basis for Reducing Nonlinear Distortion and Equalizing Response in Woofer Systems," *J. Audio Eng. Soc.,* vol. 40, pp. 675 - 691 (1992).

[19] J. Suykens, J. Vandewalle and J. van Gindeuren, "Feedback Linearization of Nonlinear Distortion in Electrodynamic Loudspeakers," *J. Audio Eng. Soc*., Vol. 43, No. 9, pp. 690-694 (1995).

[20] W. Klippel, "Direct Feedback Linearization of Nonlinear Loudspeaker Systems," *J. Audio Eng. Soc*., Vol. 46, pp. 499-507 (1995 June).

[21] H. Schurer, C. H. Slump, O.E. Herrmann, "Theoretical and Experimental Comparison of Three Methods for Compensation of Electrodynamic Transducer Nonlinearity," *Audio Eng. Soc*., Vol. 46, pp. 723-739 (1998 September).

[22] W. Klippel, "Adaptive Nonlinear Control of Loudspeaker Systems," *J. Audio Eng. Soc*. vol. 46, pp. 939 - 954 (1998).

[23] F.Y. Gao, "Adaptive Linearization of a Loudspeaker," presented at 93rd Convention of the Audio Eng. Soc., October 1 -4, 1992, San Francisco, preprint 3377.

[24] W. Klippel, "Nonlinear Adaptive Controller for Loudspeakers with Current Sensor," presented at the 106th Convention of the Audio Engineering Society, Munich, May 8-11, 1999, preprint 4864.

[25] W. A. Frank, "An Efficient Approximation to the Quadratic Volterra Filter and its Application in Real-Time Loudspeaker Linearization," *Signal Processing*, vol. 45, pp. 97-113, (1995).

[26] D. Clark, „Precision Measurement of Loudspeaker Parameters," *J. Audio Eng. Soc.* vol. 45, pp. 129 - 140 (1997 March).

[27] E. Geddes and A. Philips, " Efficient Loudspeaker Linear and Nonlinear Parameter Estimation," presented at the 91st Convention of the Audio Engineering Society, J. Audio Eng. Soc. (Abstracts), vol. 39, p. 1003 (1991 Dec.), preprint 3164.

[28] D. Clark and R. Mihelich, "Modeling and Controlling Excursion-Related Distortion in Loudspeakers," presented at the 106th Convention of the Audio Engineering Society, Munich, May 8-11, 1999, preprint 4862.

[29] D. Clark, "Amplitude Modulation Method for Measuring Linear Excursion of Loudspeakers," presented at the 89th Convention of the Audio Engineering Society, J. Audio Eng. Soc. (Abstracts), vol. 38, p. 874 (1990 Nov.), preprint 2986.

[30] G. Cibelli, A. Bellini, E. Ugolotti, "Dynamic measurements of low-frequency loudspeakers modeled by Volterra series," in *preprint 4968* presented on 106th Convention of the Audio Eng. Soc., Munich, May 8-11, 1999.

[31] M. Knudsen, "Estimation of Physical Parameters in Linear and Nonlinear Dynamic Systems, Ph. D. dissertation, Aalborg University, Department of Control Engineering, ISNN 0106-0791, AUC-CONTROL- R93 – 4010, January 1993.

[32] M. Knudsen, J.G. Jensen, V. Julskjaer and P. Rubak, "Determination of Loudspeaker Driver parameters Using a System Identification Technique," ," *J. Audio Eng. Soc*. vol. 37, No. 9.

[33] W. Klippel, "Measurement of Large-Signal Parameters of Electrodynamic Transducer," presented at the 107th Convention of the Audio Engineering Society, New York, September 24-27, 1999, preprint 5008.

[34] S. Hutt, “Loudspeaker Spider Linearity” presented at the 108th convention Audio Eng. Soc., Paris, February 19-22, 2000, preprint 5159.

[35] W. Klippel, “Distortion Analyzer – a New Tool for Assessing and Improving Electrodynamic Transducer,” presented at the 108th Convention of the Audio Engineering Society, Paris, February 19-22, 2000, preprint 5109.

VIII. APPENDIX: CASE STUDY OF WOOFER NONLINEARITIES

The large signal parameters of loudspeakers A-H have been measured in the large-signal domain characterized by the state signals in Table 2. In addition to the loudspeaker parameters given in Table 1 the following catalogue shows the nonlinear characteristics of force factor $b(x)$, stiffness $K_{MS}(x)$, inductance $L_E(x)$, resonance frequency $f_s(x)$ and total loss factor $Q_{TS}(x)$ versus displacement. The most important features related to design, behaviour, stability, source of distortion, output limiting factors and application are summarized for each driver. A second page shows the result of a driver diagnosis where the problems and imperfections are discussed in the order of their importance and conclusions for practical improvements are derived.

Measurement: Driver A

Special Design Feature • high voice coil overhang • Short cut ring is used
Dominant Source of Distortion • suspension d_C= 45 %
Stability • positive DC-displacement
Output Limiting Factor • mechanical suspension
Application • low intermodulation distortion at small amplitudes • high cost

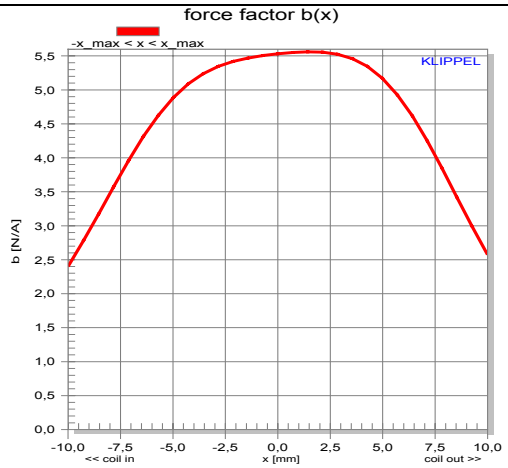

Fig. 11: Force factor versus displacement

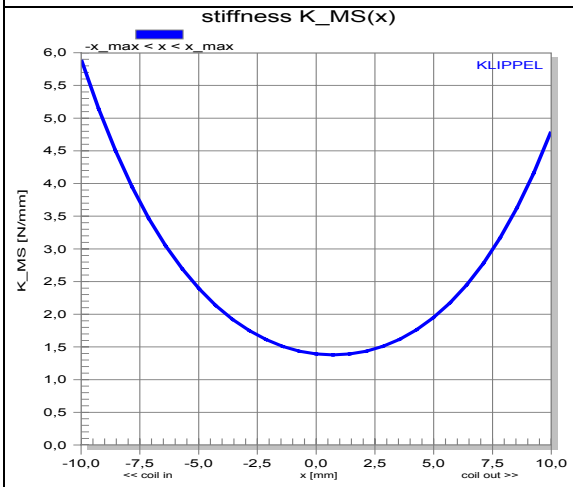

Fig. 12: Stiffness versus voice coil displacement

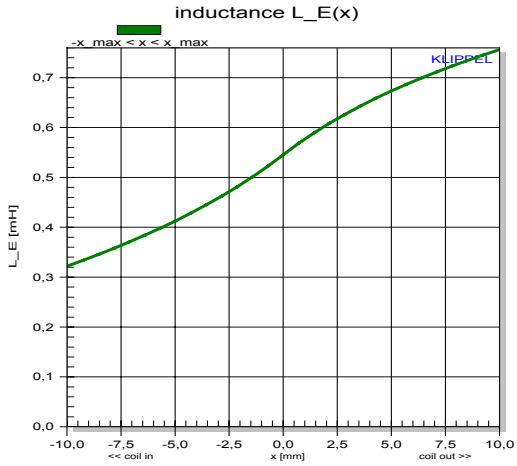

Fig. 13: Inductance versus displacement

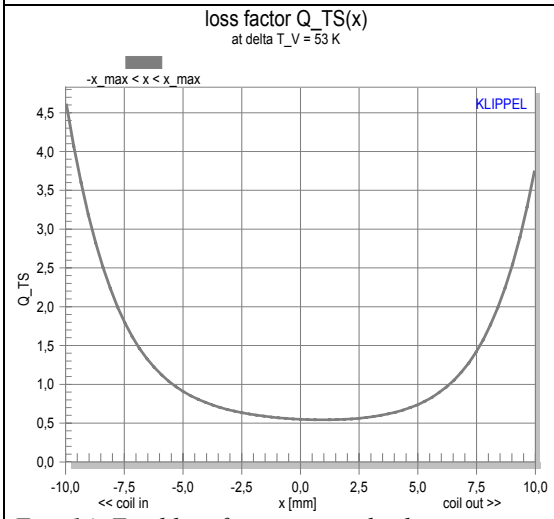

Fig. 14: Total loss factor versus displacement

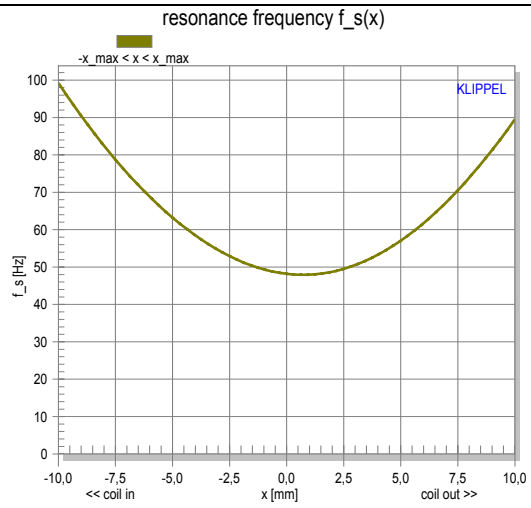

Fig. 15: Resonance frequency versus displacement

Diagnosis Driver A

Problem	Effect	Cause	Remedy
1. asymmetry $K_{MS}(x)$ $x_C(x_{peak}) \approx const.$	• instability • second- and higher-order distortion at high amplitudes • dynamic generation of a positive DC-displacement	• asymmetrical geometry of surround (half roll)	• increase x_r by 0.7 mm
2. symmetry $K_{MS}(x)$	• limits x_{max} (maybe desired) • generates low frequency distortion	• spider	• use spider with regressive role geometry
3. asymmetry $L_E(x)$	• reluctance force in positive direction • intermodulation distortion	• short cut ring causes overcompensation of inductance at negative displacement	• shift short cut ring in positive direction

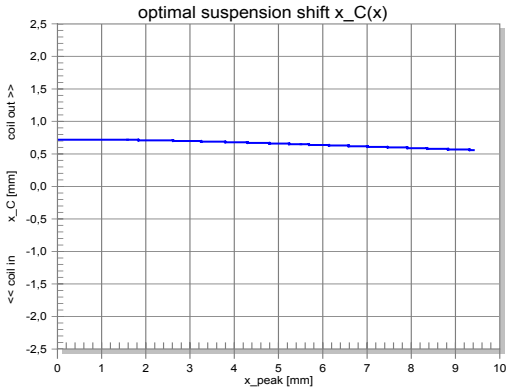

Fig. 16: Optimal working point $x_C(x_{peak})$ of suspension to give symmetry for signal amplitudes x_{peak}.

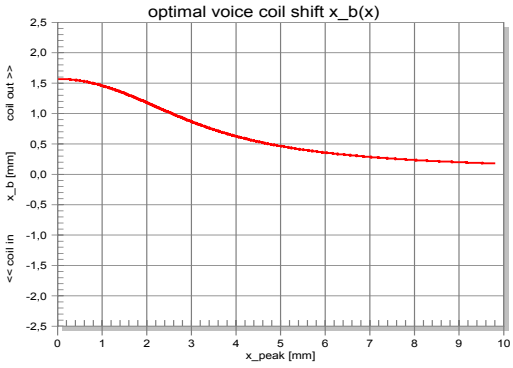

Fig. 17: Offset $x_b(x_{peak})$ of the voice coil versus signal amplitude x_{peak} required to compensate asymmetry of force factor characteristic

Measurement: Driver B

Special Design Feature • low stiffness of suspension
Dominant Source of Distortion • motor d_b=38 % • suspension d_C=29 %
Stability • positive DC-displacement for $f < f_S$ • negative DC-displacement for $f > f_s$
Problems • mechanical destruction of surround at x_{bottom} < - 7mm
Output Limiting Factor • mechanical suspension
Application • high efficient driver for sealed enclosure

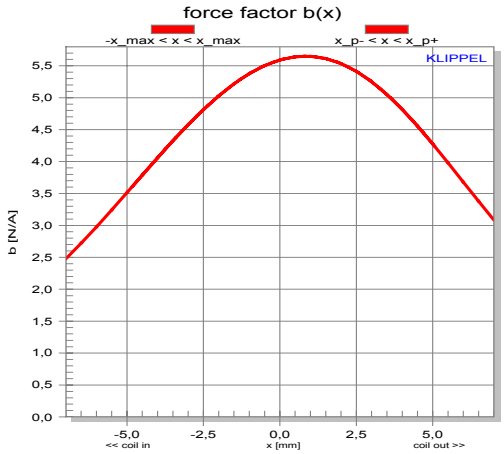

Fig. 18: Force factor versus displacement

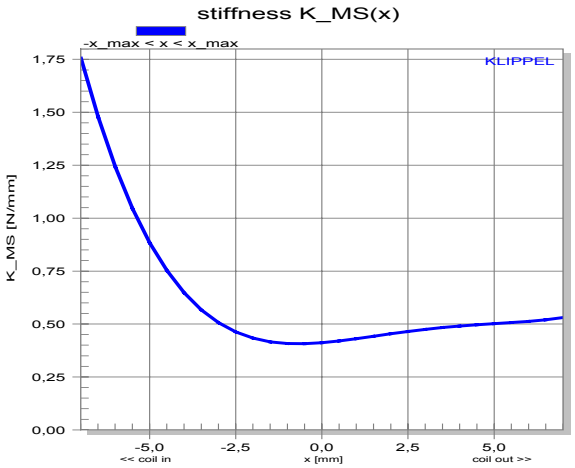

Fig. 19: Stiffness versus voice coil displacement

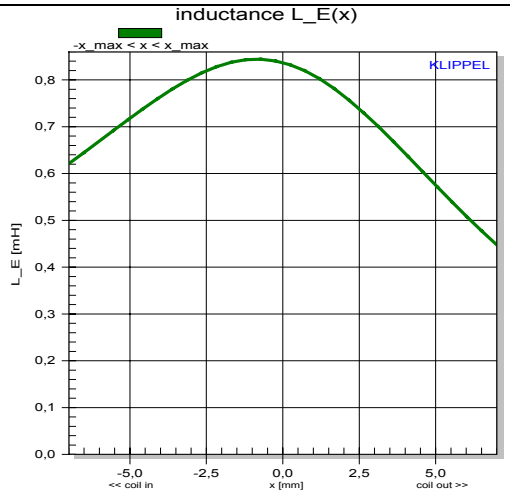

Fig. 20: Inductance versus displacement

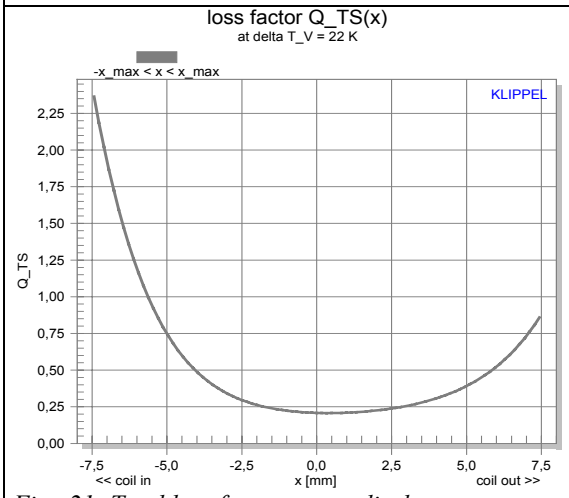

Fig. 21: Total loss factor versus displacement

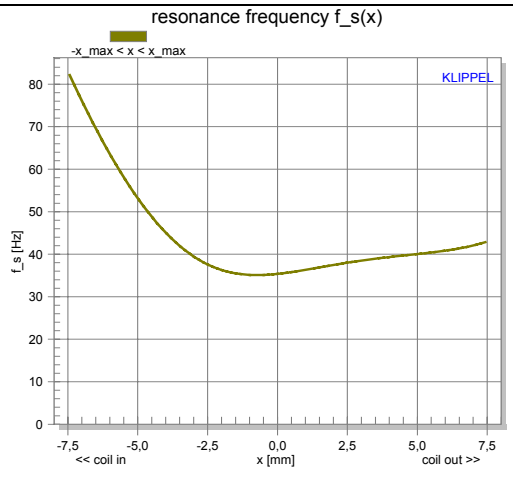

Fig. 22: Resonance frequency versus displacement

Diagnosis Driver B

Problem	Effect	Cause	Remedy
1. asymmetry $K_{MS}(x)$ • $x_C(x_{peak}) \neq const.$	• instability • second- and higher-order distortion at high amplitudes • dynamic generation of a positive dc displacement • destruction of the surround	• $x_C(x_{peak}=7$ mm) is caused by asymmetrical limiting of the surround	• increase x_r by + 2 mm
2. asymmetry $b(x)$ • $x_b(x_{peak}) \approx const.$	• instability • second- and higher-order distortion at high amplitudes • dynamic generation of DC-displacement	• voice coil rest position	• shift voice coil + 0,75 mm out
3. asymmetry $L_E(x)$	• reluctance force in negative direction • second-order intermodulation distortion at high frequencies	• no short cut ring is used	• place short cut cup above pole piece or ring at –1 mm
4. symmetry $b(x)$	• limits x_{max} • $b(x)$ generates third-order distortion in the full audio band	• after fixing K_{MS}-asymmetry the motor is the limiting part <u>not</u> the suspension	• increase voice coil height to enhance x_{max}

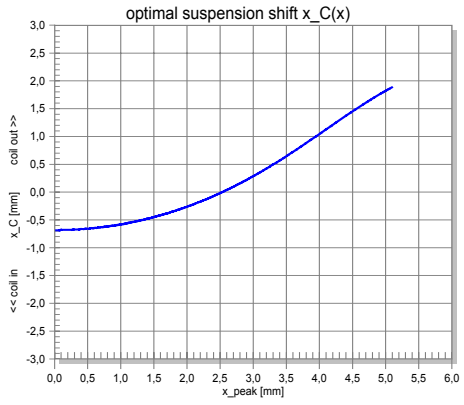

Fig. 23: Optimal working point $x_C(x_{peak})$ of suspension to give symmetry for signal amplitudes x_{peak}.

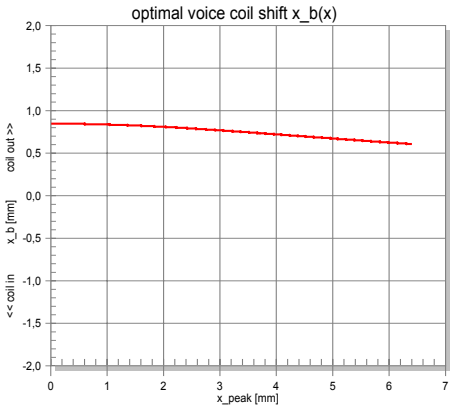

Fig. 24: Offset $x_b(x_{peak})$ of the voice coil versus signal amplitude x_{peak} required to compensate asymmetry of force factor characteristic

Measurement: Driver C

Special Design Feature
- large x_{max}
- large voice coil overhang
- large pole plate thickness (gap depth)

Dominant Source of Distortion
- suspension $d_C = 46$ %

Problem
- flux modulation

Stability
- positive DC-displacement for $f < f_s$
- negative DC-displacement for $f > f_s$

Output Limiting Factor
- mechanical suspension

Application
- vented-box system

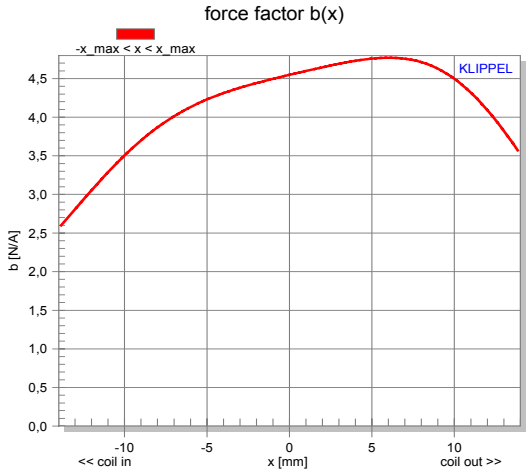

Fig. 25: Force factor versus displacement

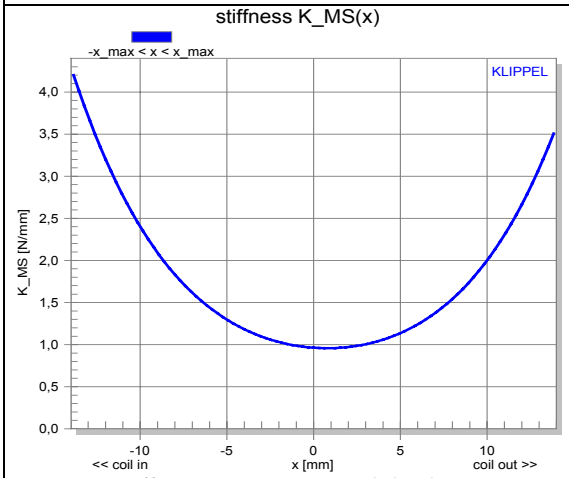

Fig. 26: Stiffness versus voice coil displacement

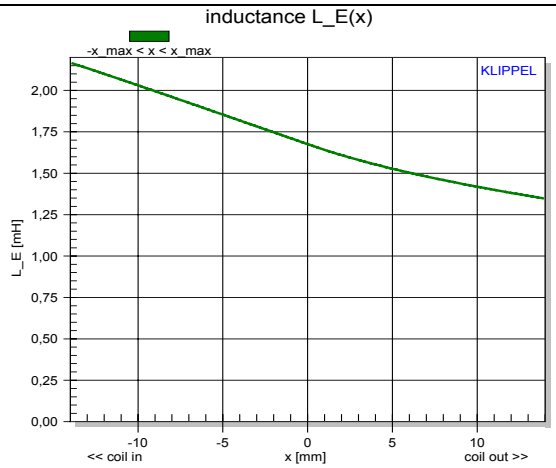

Fig. 27: Inductance versus displacement

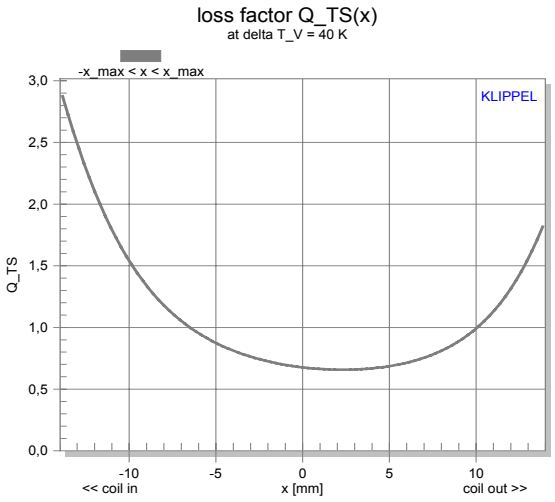

Fig. 28: Total loss factor versus displacement

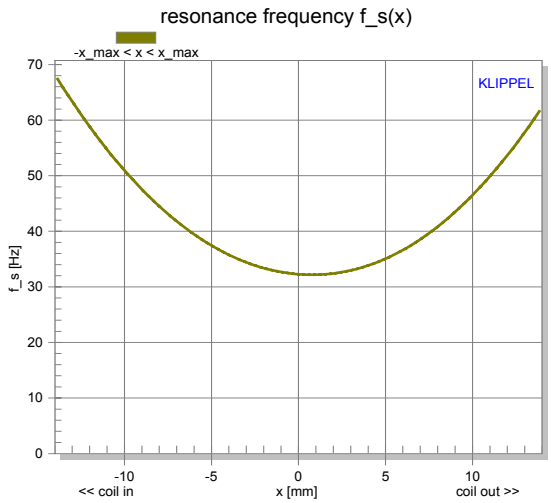

Fig. 29: Resonance frequency versus displacement

Diagnosis Driver C

Problem	Effect	Cause	Remedy
1. asymmetry *b(x)* • $x_b(x_{peak}) \neq const.$ • starting at small amplitudes	• instability • second- and higher-order distortion at high amplitudes • dynamic generation of DC-displacement	• high magnetic flux generated by alternating current in voice coil (flux modulation)	• reduce alternating flux in gap (decrease inductance, short voice coil height, reduce gap depth, reduce number of windings in gap, reduce voice coil current) • shift voice coil 2 mm out (compensates asymmetry partly)
2. asymmetry $L_E(x)$	• reluctance force in negative direction • intermodulation distortion at high frequencies	• no short cut ring is used	• place short cut ring below gap
3. symmetry $K_{MS}(x)$	• limits x_{max} • generates odd-order distortion at low frequencies	• spider	• not required since feature is used for protection • use spider with regressive role geometry
4. asymmetry $K_{MS}(x)$	• instability • second-order distortion at high amplitudes • dynamic generation of a positive DC-displacement	• asymmetrical geometry of surround (half roll)	• add 0.7 mm to x_r to shift surround in positive direction

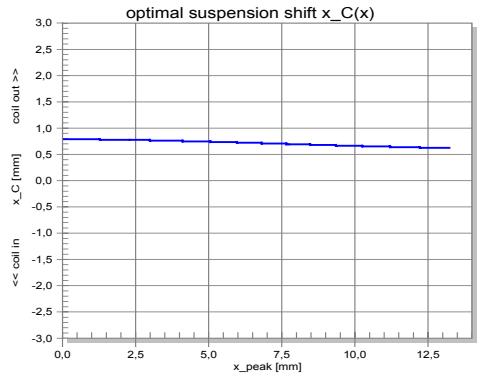

Fig. 30: Optimal working point $x_C(x_{peak})$ of suspension to give symmetry for signal amplitudes x_{peak}.

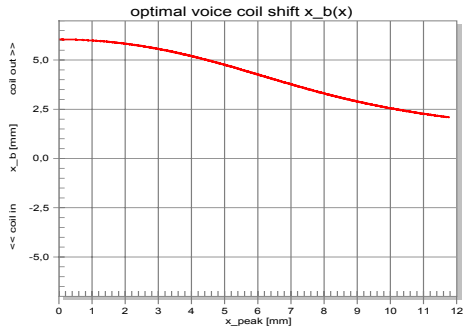

Fig. 31: Offset $x_b(x_{peak})$ of the voice coil versus signal amplitude x_{peak} required to compensate asymmetry of force factor characteristic

Measurement: Driver D

Special Design Feature • linear motor • large voice coil overhang
Dominant Source of Distortion • suspension d_C = 78 %
Stability • negative DC-displacement
Output Limiting Factor • mechanical suspension
Application • medium efficiency • vented enclosure • low intermodulation distortion

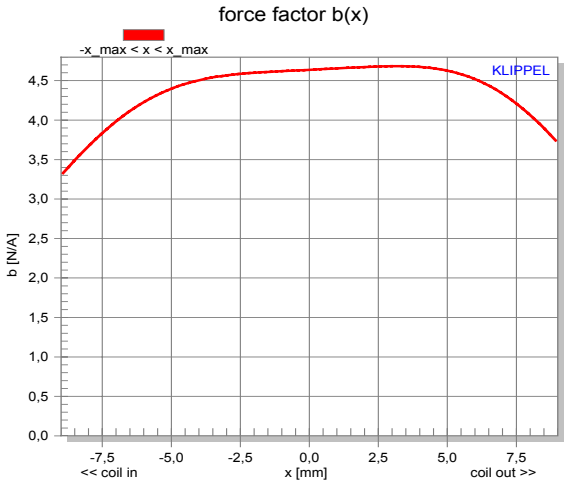

Fig. 32: Force factor versus displacement

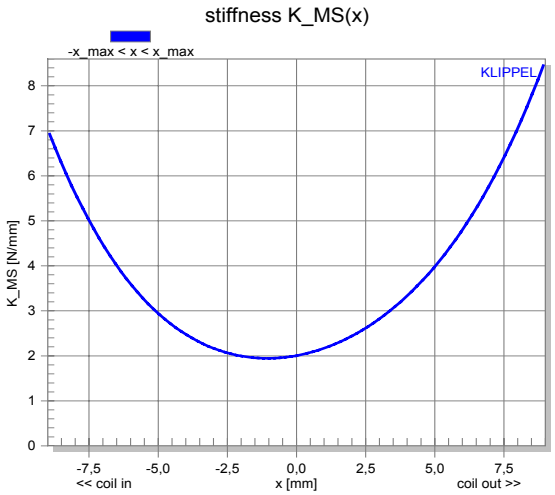

Fig. 33: Stiffness versus voice coil displacement

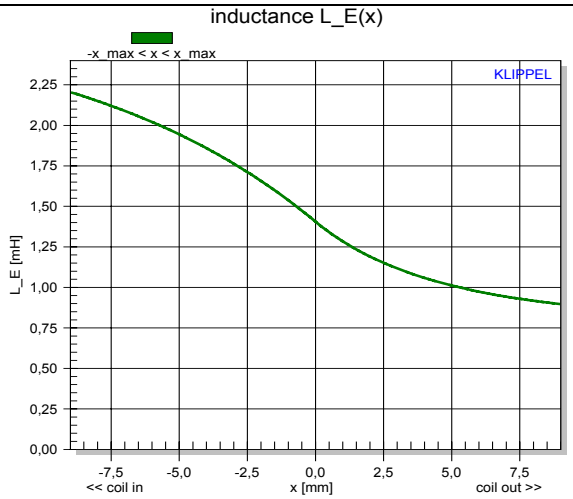

Fig. 34: Inductance versus displacement

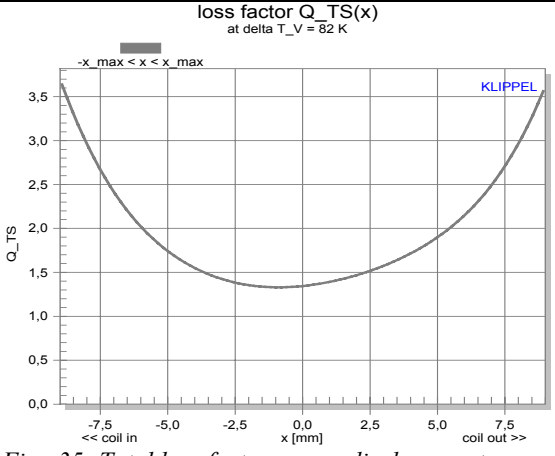

Fig. 35: Total loss factor versus displacement

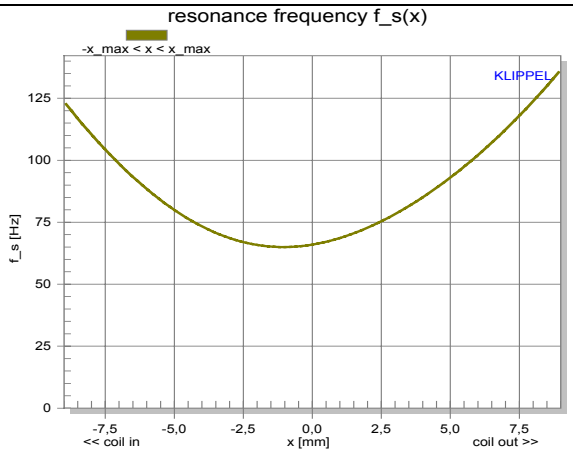

Fig. 36: Resonance frequency versus displacement

Diagnosis Driver D

Problem	Effect	Cause	Remedy
1. asymmetry $K_{MS}(x)$ • starting at small amplitudes	• instability • second- and higher-order distortion at high amplitudes • negative DC-displacement	• asymmetrical geometry of spider (pot form) • asymmetrical geometry of surround (half roll)	• reduce x_r by - 1 mm
2. asymmetry $L_E(x)$	• reluctance force in negative direction • intermodulation distortion at higher frequencies	• no short cut ring is used	• place short cut ring below gap
3. symmetry $K_{MS}(x)$	• limits x_{max} • generates low frequency distortion • protects the voice coil former	• spider	• use spider with regressive role geometry
4. asymmetry $b(x)$ • $x_b(x_{peak}) \neq const.$ • starting at small amplitudes	• dynamic generation of DC- displacement	• high magnetic flux generated by alternating current in voice coil (flux modulation)	• reduce alternating flux in gap (decrease inductance, short voice coil height, reduce gap depth, reduce number of windings in gap, reduce voice coil current) • shift voice coil 2 mm out (partly compensates asymmetry)

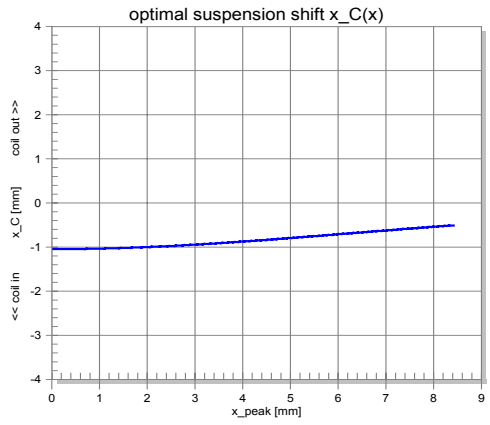

Fig. 37: Optimal working point $x_C(x_{peak})$ of suspension to give symmetry for signal amplitudes x_{peak}.

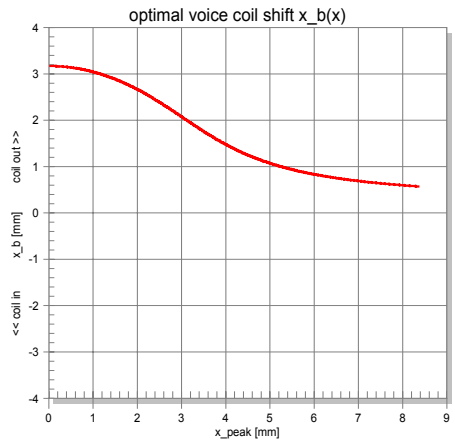

Fig. 38: Offset $x_b(x_{peak})$ of the voice coil versus signal amplitude x_{peak} required to compensate asymmetry of force factor characteristic

Measurement: Driver E

Special Design Feature
- low stiffness of suspension
- high efficient motor
- low inductance
- equal length configuration

Dominant Source of Distortion
- motor d_b = 68 %

Stability
- minor generation of DC-displacement

Problem
- broad band intermodulation distortion

Output Limiting Factor
- force factor of motor

Application
- high efficiency
- low weight & low cost

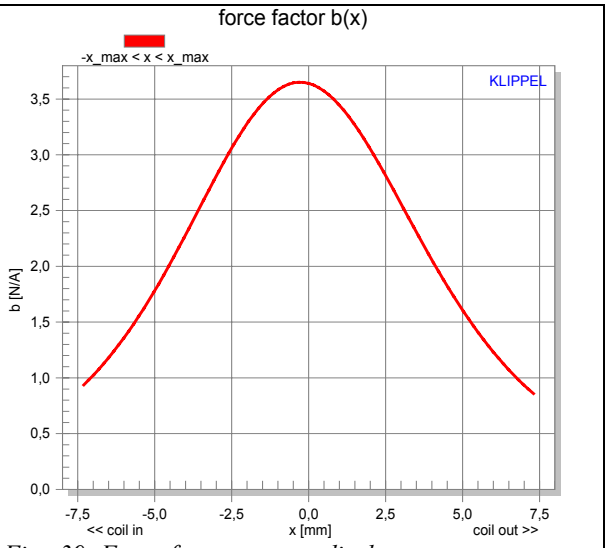

Fig. 39: Force factor versus displacement

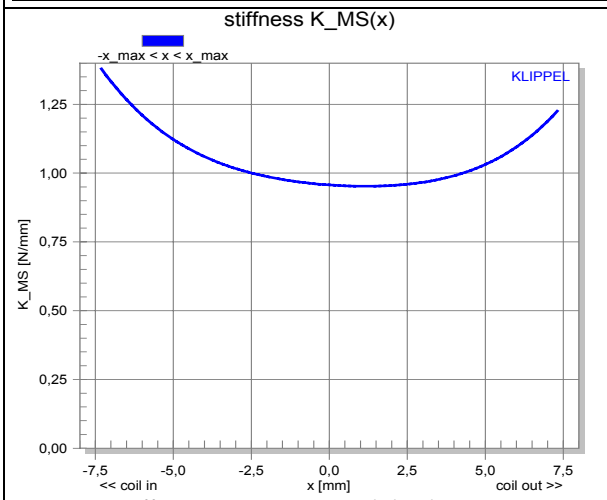

Fig. 40: Stiffness versus voice coil displacement

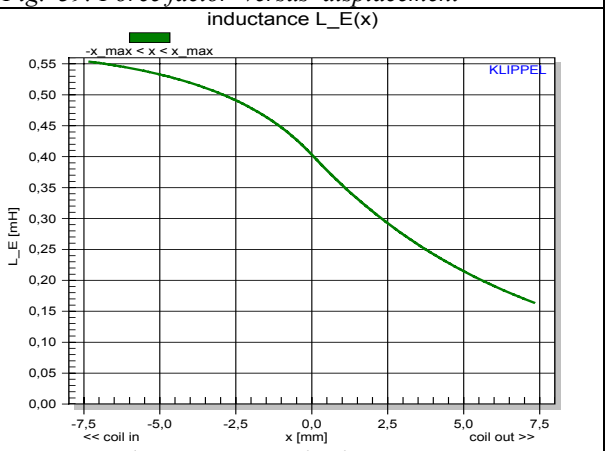

Fig. 41: Inductance versus displacement

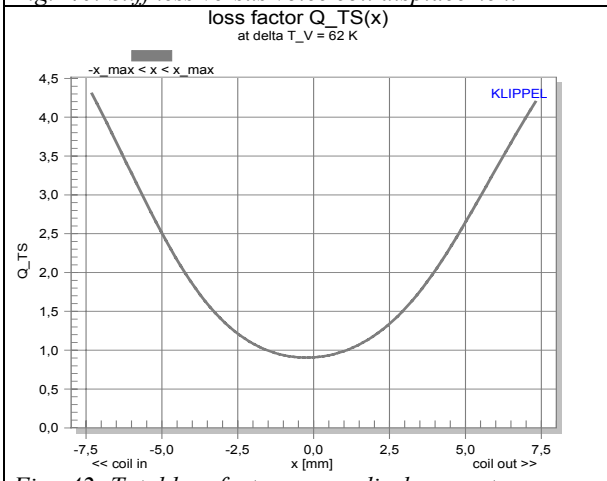

Fig. 42: Total loss factor versus displacement

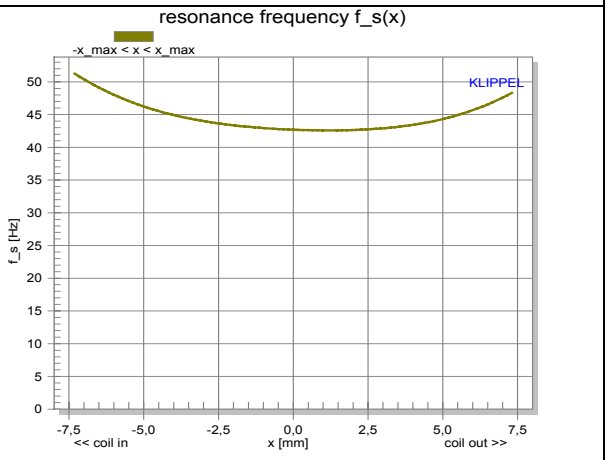

Fig. 43: Resonance frequency versus displacement

Diagnosis Driver E

Problem	Effect	Cause	Remedy
1. symmetry *b(x)* • starting at small amplitudes	• limits x_{max} • intermodulation distortion in full audio band	• equal length configuration	• not required since property gives maximal efficiency • increase voice coil height
2. asymmetry $L_E(x)$	• reluctance force in negative direction • intermodulation distortion at high frequencies	• no short cut ring is used	• place short cut ring below gap
3. asymmetry $K_{MS}(x)$ • starting at small amplitudes	• positive DC-displacement generated by suspension deteriorates motor symmetry • second-order distortion at low frequencies	• asymmetrical geometry of surround (half roll)	• increase x_r by +1 mm

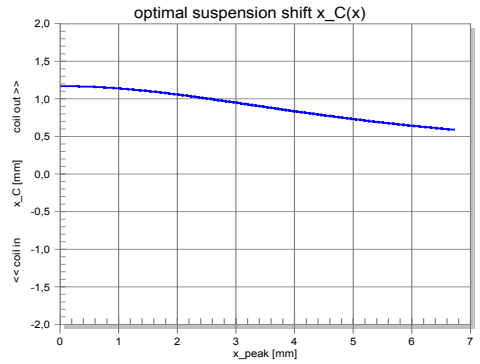

Fig. 44: Optimal working point $x_C(x_{peak})$ of suspension to give symmetry for signal amplitudes x_{peak}.

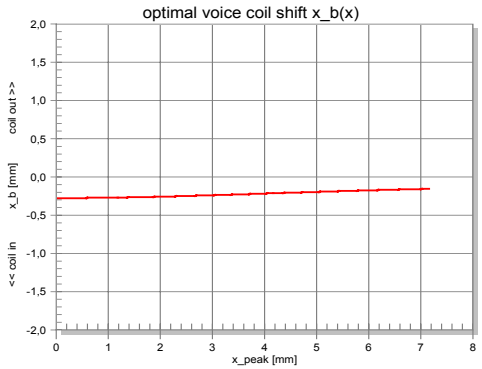

Fig. 45: Offset $x_b(x_{peak})$ of the voice coil versus signal amplitude x_{peak} required to compensate asymmetry of force factor characteristic

Measurement: Driver F

Special Design Feature
- equal length configuration

Dominant Source of Distortion
- motor $d_b = 49$ %
- suspension $d_C = 34$ %

Stability
- positive DC-displacement for $f < f_s$
- negative DC-displacement for $f > f_s$

Output Limiting Factor
- force factor
- stiffness

Application
- high efficiency
- sealed enclosure
- low cost & weight

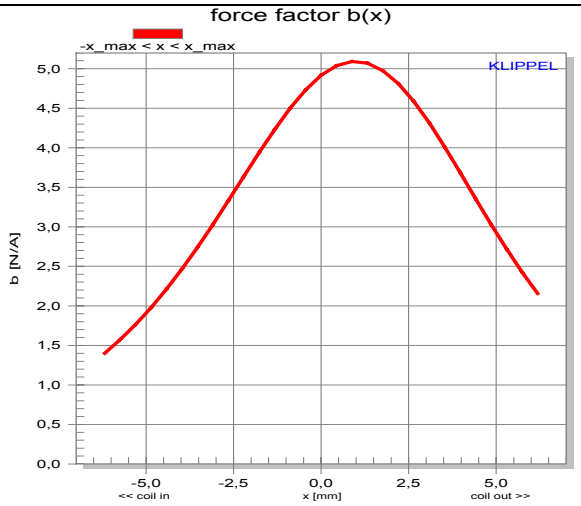

Fig. 46: Force factor versus displacement

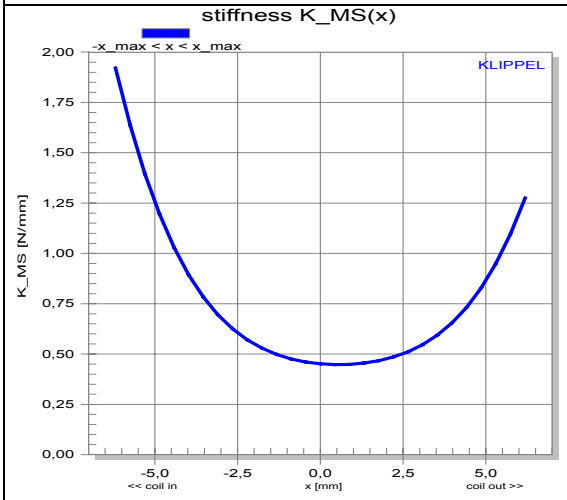

Fig. 47: Stiffness versus voice coil displacement

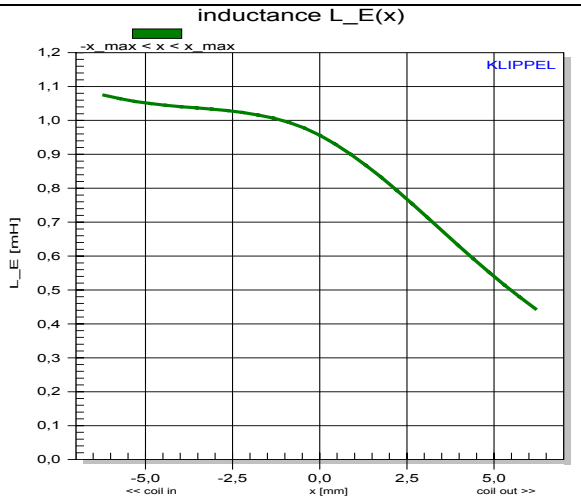

Fig. 48: Inductance versus displacement

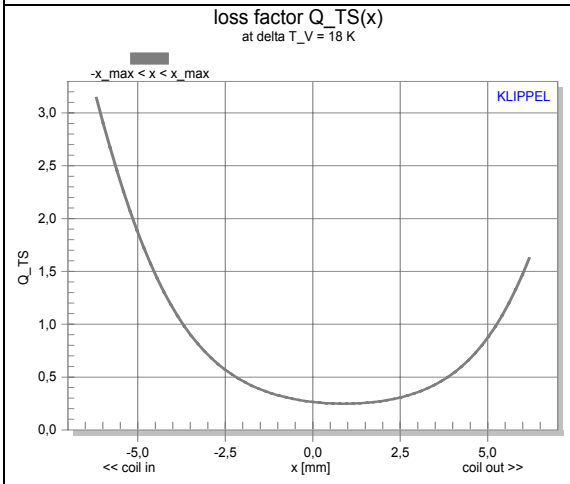

Fig. 49: Total loss factor versus displacement

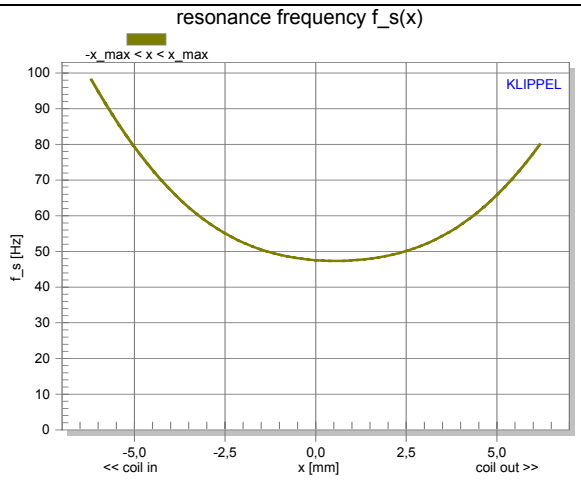

Fig. 50: Resonance frequency versus displacement

Diagnosis Driver F

Problem	Effect	Cause	Remedy
1. asymmetry *b(x)* • $x_b(x_{peak}) \approx$ const.	• instability • second-order intermodulation in full audio band • dynamic generation of a DC displacement	• voice coil position	• shift voice coil + 1,2 mm out
2. asymmetry $K_{MS}(x)$	• positive DC-displacement generated by suspension deteriorates motor symmetry • second-order distortion at low frequencies	• asymmetrical geometry of surround (half roll)	• increase x_r by + 0.5 mm
3. symmetry $K_{MS}(x)$ • rapid increase at high amplitudes	• limits x_{max} • generates low frequency distortion • destruction of surround	• surround is limiting	• use harder spider to protect surround • increase size of surround
4. asymmetry $L_E(x)$	• reluctance force in negative direction • intermodulation distortion at high frequencies	• no short cut ring is used	• place short cut ring below gap
5. symmetry *b(x)* • starting at small amplitudes	• limits x_{max} • odd-order intermodulation in full audio band	• equal length configuration	• not required since property gives maximal efficiency • increase voice coil height

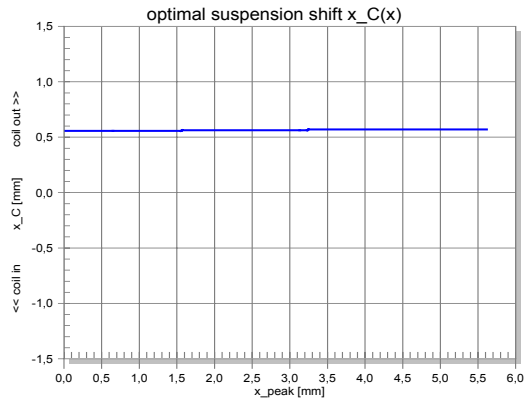

Fig. 51: Optimal working point $x_C(x_{peak})$ of suspension to give symmetry for signal amplitudes x_{peak}.

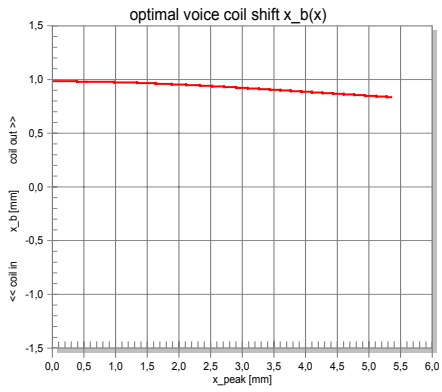

Fig. 52: Offset $x_b(x_{peak})$ of the voice coil versus signal amplitude x_{peak} required to compensate asymmetry of force factor characteristic

Measurement: Driver G

Special Design Feature
- large voice coil overhang
- large pole plate thickness (gap depth)

Dominant Source of Distortion
- suspension $d_C = 46\ \%$

Problem
- suspension limits at negative displacement

Stability
- positive DC-displacement for $f < f_s$

Output Limiting Factor
- mechanical suspension

Application
- medium efficiency
- vented enclosure
- low intermodulation distortion

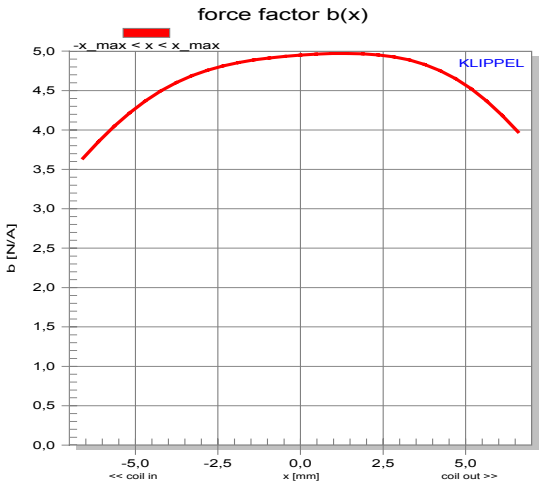

Fig. 53: Force factor versus displacement

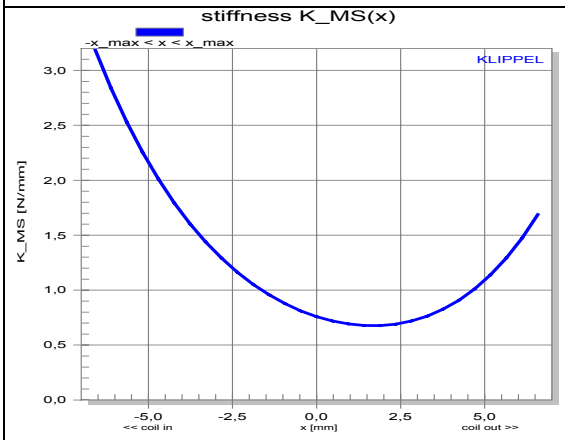

Fig. 54: Stiffness versus voice coil displacement

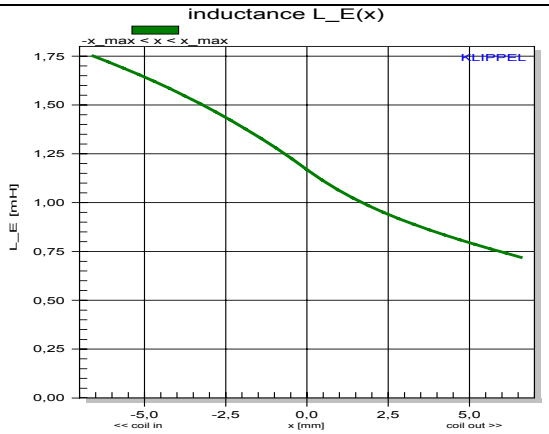

Fig. 55: Inductance versus displacement

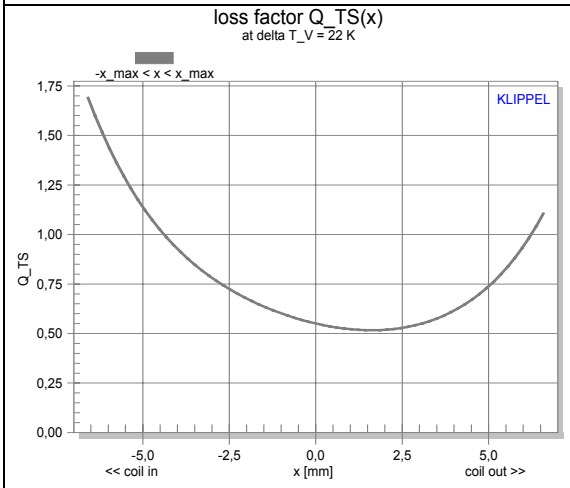

Fig. 56: Total loss factor versus displacement

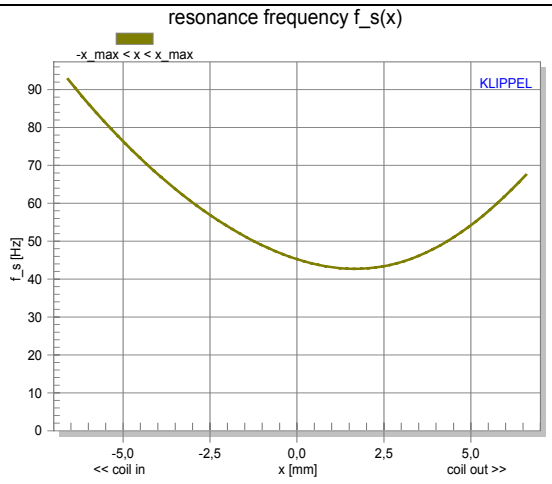

Fig. 57: Resonance frequency versus displacement

Diagnosis Driver G

Problem	Effect	Cause	Remedy
1. asymmetry $K_{MS}(x)$ $x_C(x_{peak}) \neq const.$	• positive DC-displacement generated by suspension deteriorates motor symmetry • second-order distortion at low frequencies	• geometry of spider (pot form)	• use spider with flat geometry • increase x_r by 1.5 mm might be helpful for compensating spider asymmetry
2. symmetry $K_{MS}(x)$ • early increase at small amplitudes	• limits x_{max} • odd-order distortion at low frequencies	• spider is limiting	• use softer spider with regressive roll geometry
3. asymmetry $L_E(x)$	• reluctance force in negative direction • intermodulation at high frequencies	• no short cut ring is used	• place short cut ring below gap

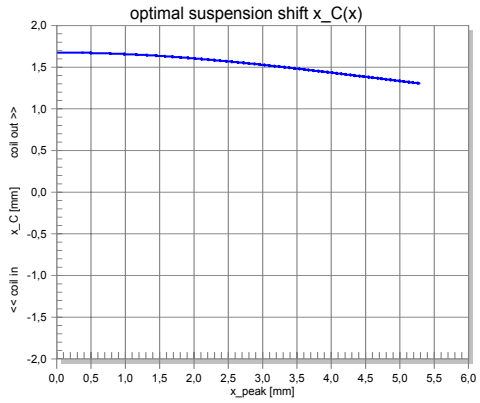

Fig. 58: Optimal working point $x_C(x_{peak})$ of suspension to give symmetry for signal amplitudes x_{peak}.

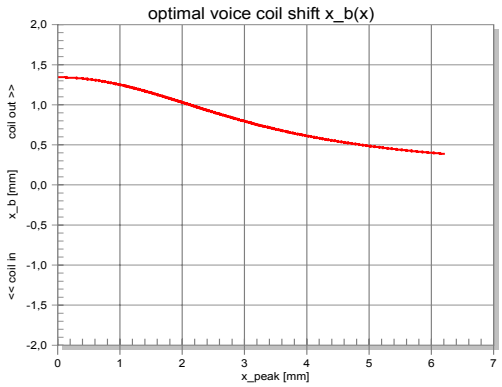

Fig. 59: Offset $x_b(x_{peak})$ of the voice coil versus signal amplitude x_{peak} required to compensate asymmetry of force factor characteristic

Measurement: Driver H

Special Design Feature
- large voice coil height
- large pole plate thickness (gap depth)
- multi-layer voice coil

Dominant Source of Distortion
- inductance $d_L = 36$ %

Problem
- voice coil hits back-plate

Stability
- positive DC-displacement for $f < f_s$
- negative DC-displacement for $f > f_s$

Output Limiting Factor
- moving capability of voice coil

Application
- subwoofer to avoid intermodulation distortion
- sealed enclosure

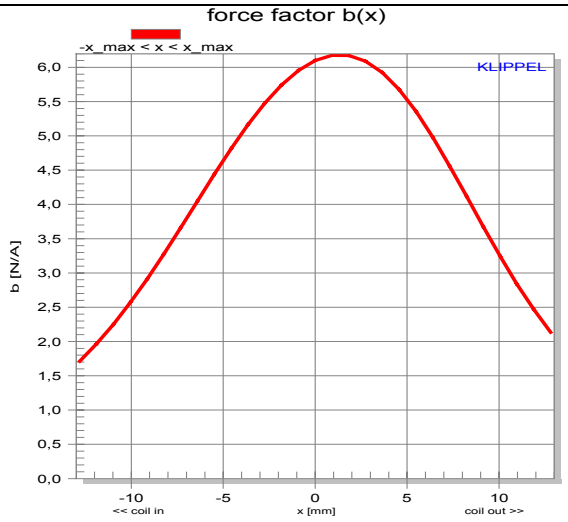

Fig. 60: Force factor versus displacement

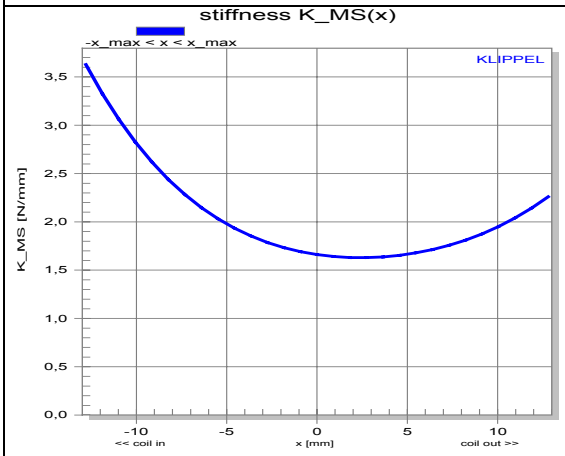

Fig. 61: Stiffness versus voice coil displacement

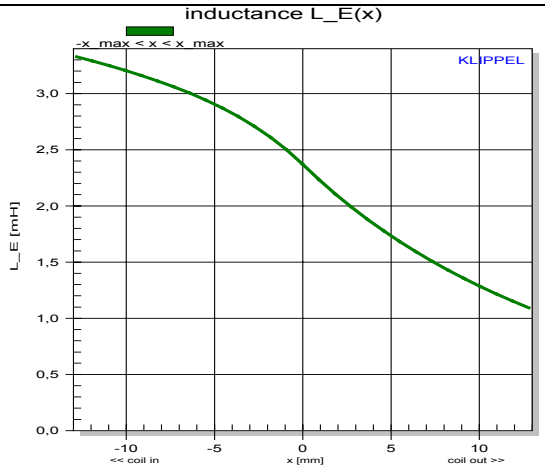

Fig. 62: Inductance versus displacement

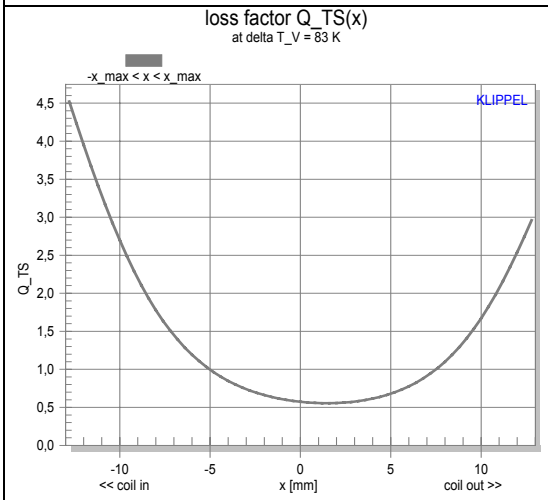

Fig. 63: Total loss factor versus displacement

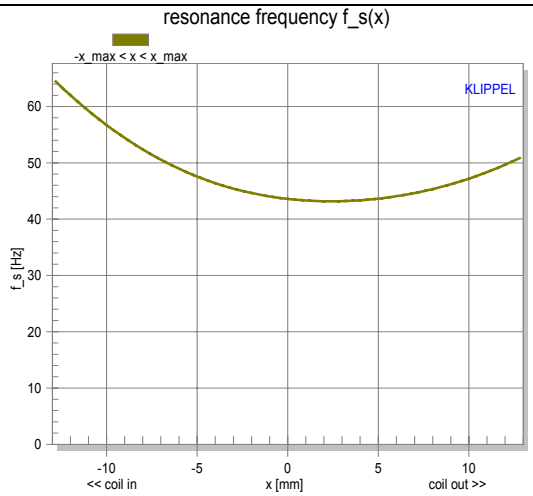

Fig. 64: Resonance frequency versus displacement

Diagnosis Driver H

Problem	Effect	Cause	Remedy
1. voice coil hits back-plate	• distortion in acoustic output starting suddenly • destruction of the voice coil former	• suspension to soft • not enough free space of movement	• use spider with higher stiffness • use spider with symmetrical stiffness characteristic • increase height of magnet
2. asymmetry $L_E(x)$	• reluctance force in negative direction • substantial intermodulation distortion at higher frequencies	• high value of inductance but no short cut ring is used	• place short cut ring below gap
3. asymmetry $K_{MS}(x)$	• positive DC-displacement generated by suspension deteriorates motor symmetry	• geometry of spider (pot form) • limiting of surround at negative displacement	• increase x_r by + 2.5 mm
4. asymmetry $b(x)$ • $x_b(x_{peak}) \approx$ const.	• instability • second-order distortion at high amplitudes • dynamic generation of a DC displacement	• voice coil position	• shift voice coil + 1 mm out

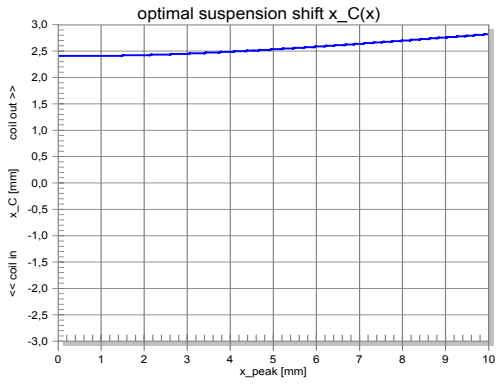

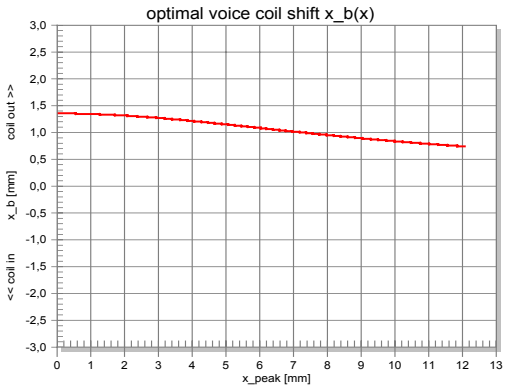

Fig. 66: Offset $x_b(x_{peak})$ of the voice coil versus signal amplitude x_{peak} required to compensate asymmetry of force factor characteristic